Thesis/
Reports
Massman,
W. J.

Final Report
The California Ozone Deposition Experiment 1991
(CODE91)

Final Report

The California Ozone Deposition Experiment 1991 (CODE91)*

by

William J. Massman

USDA/Forest Service

240 West Prospect

Fort Collins, Colorado 80526

for

The San Joaquin Valley Air Quality Study (SJVAQS)

and

The Atmospheric Utility Signatures, Predictions, and Experiments (AUSPEX)

and

The SJVAQS/AUSPEX Regional Model Adaption Project (SARMAP)

June, 1996

* The statements and conclusions in this report are those of the author and not necessarily those of the ARB, the JPA, the San Joaquin Valley Air Quality Study Policy Committee, the SARMAP sponsors, their employees or members. The mention of commercial products, their source or their use in connection with material reported herein is not to be construed as actual or implied endorsement of such products.

Table of Contents

Executive Summary

Chapter I - Sensitivity analysis and initial assessment of the Regional Acid Deposition Model dry deposition module

Chapter II - Use of a Regional Acid Deposition Model-like dry deposition module for modeling the dry deposition of ozone in the San Joaquin Valley: Recommendation based on the site specific CODE91 data

Chapter III - An evaluation of the regional acid deposition model surface module for ozone uptake at three sites in the San Joaquin Valley of California

Chapter IV - Surface conductances for ozone uptake derived from aircraft eddy correlation data

Chapter V - Estimating canopy conductance to ozone uptake from observations of evapotranspiration at the canopy scale and at the leaf scale

Chapter VI - Final data report for the California ozone deposition experiment

Chapter VII - Preliminary investigation of the effects of Nitric Oxide fluxes upon the California Ozone Deposition Experiment ozone flux data

Executive Summary

This report is a collection of seven independently written preliminary reports and published studies that document the findings of the USDA/Forest Service's contribution to the California Ozone Deposition Experiment (CODE). In general the seven studies evaluate different near-surface formulations of dry deposition using CODE data, quantify the uncertainties associated with the measurement and modeling of dry deposition, and recommend a modified formulation of dry deposition for modeling the air quality of the San Joaquin Valley.

In CODE, vertical fluxes of ozone were measured by the eddy-correlation method using tower-based instruments at three sites representing the most prevalent land use categories, which are rangeland, cotton, and vineyards. Additional eddy-correlation measurements were made with an aircraft confirming the tower-based results and providing further information on ozone uptake for additional crops. Agriculture and rangeland represent 24 and 14 percent of the total modeling domain and most of the nonurban area of the San Joaquin Valley floor.

Ozone fluxes were interpreted as ozone uptake at the surface and normalized by ozone concentration to give corresponding deposition velocities. Generally, ozone deposition velocities for irrigated crops were similar in magnitude and diurnal variation. The daytime velocities over irrigated crops were much higher and ranged between those observed for vineyards and orchards (low) and cotton and corn (high). Deposition velocities for dry rangeland were much lower than for irrigated crops and nearly the same for day and night.

By comparing observed and modeled dry deposition velocity, a model of pollutant deposition to plants and soil, previously developed for other regions and applied to the San Joaquin Valley, was determined inappropriate. This model incorrectly assumed that deposition decreased markedly for temperatures commonly seen during ozone episodes in the San Joaquin Valley. It assumed maximal deposition at 20°C (68°F), reduced deposition by 25 percent at 30°C (86°F), and completely curtailed deposition for temperatures at or above 40°C (104°F). No such temperature dependence was observed. This model also incorrectly represented the response of surface conductance and deposition velocity to sunlight, increasing surface conductance and deposition too quickly in response to sunlight. In general, this previously used model overestimated maximum daytime deposition rates by 50 percent for irrigated agricultural areas and by a factor of five or more for rangeland.

The deposition model was modified to provide consistency with the observed relationships between ozone deposition rates and environmental variables. The changes removed the inappropriate temperature dependence for surface conductance, provided a nearly linear response to sunlight intensity, and generally reduced estimated daytime and nighttime deposition rates over irrigated crops by about 35 percent and reduced estimated daytime deposition rates over dry rangeland by about eighty percent. Compared to previous estimates, these modifications reduce the predicted spatially averaged daytime deposition velocity for the SARMAP domain by about 35 percent, but do not significantly change the predicted spatially averaged nightime deposition velocity.

Although the new model of surface deposition was quite successful at simulating the observed deposition velocities, one discrepancy was unexplained. The observed ozone fluxes

at the CODE cotton site were consistently greater than at the vineyard site even though the evapotranspiration (ET) rates were comparable. If ozone deposition is largely controlled by plant stomata then comparable ET rates suggest that the ozone fluxes should also be comparable at both sites. One explanation for this difference is that high cotton crop fertilization causes nitrogen oxide (NO) soil emissions to be much higher at the cotton site than the vineyard site. However, measurements of NO emission rates from soils obtained after CODE indicate that the soil efflux rates of NO were probably not high enough to cause the discrepancy. Since the time of the work discussed in this report two other explanations have been suggested. The first is that there is a local source of NO such as an irrigation pump (Mahrt et al., 1995, J. Geophys. Res., 100: 23,125-23,131). The second is that a (presently unknown) photochemical reaction taking place on the leaf cuticle is another sink of ozone (Coe et al., 1995, Atmospheric Environment, 29: 1413-1423). Presently there is no satisfactory explanation. The remainder of this summary outlines the main theme and the findings of each chapter.

Chapter I

Two separate near-surface dry deposition formulations or modules, BDRYDEP and MODDEP2, are discussed. MODDEP2 is evaluated for sensitivity to input parameters and potential measurement related errors. The results of this preliminary analysis suggest that the modeled temperature response of the plants' stomatal uptake of ozone is incorrectly formulated for the San Joaquin Valley and that both plant and aerodynamic components of the modeled dry deposition need detailed, separate evaluations.

Chapter II

Wesely's (1989; Atmospheric Environment, 23: 1293-1304) near-surface parameterization for dry deposition is evaluated using the CODE data. Model performance, quality of the CODE data used for model input, and model uncertainties are discussed. The significant differences between the ozone uptake rates of a cotton canopy and a grape canopy suggest that including all agricultural crops into one surface type could introduce significant errors into model calculations of dry deposition rates. An improved model of plant ozone uptake is developed from the CODE data and recommendations are made for improving the performance of the original Wesely model.

Chapter III

Although this published version of the preceeding chapters shares many of the same goals and results, it differs in several important ways. First, the final CODE data set is used for the published analysis; in the preceding chapters the CODE data were still undergoing evaluation and error checking. Second, the model of ozone uptake by plants developed in this chapter is simpler than the one developed in the preceeding chapter. Third, this published analysis contains a detailed discussion of the influence of dew on dry deposition rates. An important conclusion is that, contrary to most models, ozone uptake rates are not necessarily reduced by dew.

Chapter IV

This chapter, published in Atmospheric Environment, uses aircraft data to estimate

surface ozone conductances for a variety of crops throughout the San Joaquin Valley. The study confirms that tower-based and aircraft-based surface conductance estimates were comparable and extends the tower-based surface conductance estimates to a larger area of the valley, thereby increasing the data base for modeling purposes. The aircraft-derived and the tower-derived surface conductances show the same range of variability for agricultural crops. In general, the measured ozone flux over cotton is higher than over other crops in the San Joaquin Valley.

Chapter V

This chapter, published in Global Change Biology, compares the canopy conductances for water vapor to those for ozone uptake, and addresses questions about scaling from a leaf-level measurement of stomatal conductance to a canopy-level conductance. The observation made in Chapter IV (Fig. 1), that the ozone flux over cotton is much higher than over grape even though the evapotranspiration rates were comparable for both canopies, motivated this study. Similar evapotranspiration rates suggest similar canopy conductances, whereas differing ozone fluxes suggest different canopy conductances. A possible explanation for these results is that because more fertilizer is applied to cotton, soil NO emissions are probably much larger from the cotton crop than from the grape site. These emissions from the cotton crop may be large enough to explain why ozone fluxes are much higher over cotton than over grape. This study also suggests that the grape canopy may be suffering from ozone induced stress and that it may be possible to diagnose this type of stress using the eddy covariance approach.

Chapter VI

This chapter documents the final CODE data set and discusses the screening procedures and corrections used in arriving at the final data set.

Chapter VII

This final chapter reviews the published sources of NO emissions from soils within the San Joaquin Valley and NO uptake rates by plants. As in Chapter V, the results presented in this chapter suggest that, in addition to uptake by plants, emissions of NO from soils may be high enough to act as a significant sink for ozone destruction. However, as mentioned in the Executive Summary at present there is no fully satisfactory explanation for why ozone fluxes are significantly higher over cotton relative to the grape vineyard or other agricultural crops.

Chapter I

Sensitivity Analysis and Initial Assessment of the RADM Dry Deposition Module

PURPOSE

The San Joaquin Valley Air Quality Study (SJVAQS) is a field measurement and computer modeling study of photochemical air pollution in the San Joaquin Valley of California. One of the goals of the SJVAQS is to improve modeling estimates of dry deposition of ozone. To accomplish this, the California Ozone Deposition Experiment (CODE) performed field measurements in July and early August of 1991. The CODE data are used here to evaluate the surface layer formulation used by the Regional Acid Deposition Model (RADM) to describe ozone destruction. This chapter documents an initial evaluation of this module using some of the CODE data and makes a preliminary assessment that the surface-layer formulation presently used in the module requires modification for modeling ozone deposition in the San Joaquin Valley.

However, this chapter does not give specific recommendations for improving the surface-layer parameterizations; these are in the next chapter. Also, comparisons made between observations and model predictions are made for one specific site and one specific plant type; however, the model is designed to operate on a much larger horizontal scale and for more than one type of plant cover. Therefore, the model and data comparisons made are preliminary only and part of a continuing study.

INTRODUCTION

The RADM dry deposition module (BDRYDEP) is designed to simulate the diurnal course of the deposition velocity (v_d) for a variety of gaseous pollutants. Consequently, BDRYDEP predicts dry deposition velocities over a grid box in a mesoscale model. MODDEP2 is a deposition model used to calibrate dry deposition parameters at a specific site. BDRYDEP and MODDEP2 share similar parameterization for the canopy component of the deposition velocity, but they differ considerably in how they parameterize the aerodynamic and plant quasi-laminar boundary layer components. Because MODDEP2 is executed independently of RADM, it was practical to evaluate MODDEP2 (rather than BDRYDEP) against the CODE observations.

This chapter evaluates the difference between MODDEP2 and BDRYDEP. The results of this evaluation can then be interpreted and extended to BDRYDEP. To simulate deposition velocity, BDRYDEP and MODDEP2 parameterize the aerodynamic resistance (r_a), plant canopy's quasi-laminar boundary layer resistance (r_b), and surface resistance (r_s). r_a describes the transfer of pollutants by turbulent atmospheric motions and is largely determined by near-surface atmospheric stability and surface roughness. r_b provides for the molecular diffusion of gaseous and/or particulate pollutants through the boundary layer of plant leaves. This resistance has both aerodynamic and plant related aspects, and is dependent upon the particular pollutant being considered. The surface resistance parameterizes the vegetation and soil properties.

In BDRYDEP (the RADM dry deposition module), r_s is comprised of several other resistances that depend upon the type of the vegetation, its phenology or growth stage, and the presence or absence of moisture on the plant leaves (Wesely, 1989). These three resistances are related to v_d as:

$$v_d = (r_a + r_b + r_s)^{-1} \tag{1}$$

Specific formulations for the resistances used in BDRYDEP are discussed by Byun (1991). Since BDRYDEP is used within a larger mesoscale meteorological model, r_a is parameterized to reflect the turbulent exchange between the surface and a model height of about 40m above that surface. However, the CODE data used in this report are limited to heights much nearer the surface, therefore the following formulation for r_a is used in this report:

$$r_a = [\log(z/z_0) - \psi_m(z/L)][\log(z/z_0) - \psi_c(z/L)]/k^2u \tag{2}$$

where z = height above the surface, u = horizontal wind speed, k (=0.4) is the von Karman constant, L = Monin-Obukhov length for atmospheric stability, ψ_m and ψ_c are stability functions, and z_0 = surface roughness length. In this report, the distinction between r_a in equation (2) and r_a in BDRYDEP is unimportant, and is discussed in Chapter III. BDRYDEP parameterizes r_b as:

$$r_b = kB_{0_3}^{-1}/ku_*$$

where u_* = friction velocity as determined in the model (Byun, 1990) and kB_{03}^{-1} is a vegetation/pollutant related parameter (Massman, 1987). This report uses a slightly different formulation for r_b given as:

$$r_b = kB_{0_3}^{-1}[\log(z/z_0) - \psi_m(z/L)]/k^2u \quad (3)$$

As with r_a above, this formulation for r_b is consistent with the BDRYDEP fomulation and differences are insignificant. In BDRYDEP $kB_{0_3}^{-1}$ has a constant value of 2.83; however, this specific value is probably more appropriate for SO_2 than ozone (Wesely, 1989), and may slightly overestimate $kB_{0_3}^{-1}$. Furthermore, $kB_{0_3}^{-1}$ is not necessarily a constant, but is also a function of the structure of the plant canopy (Massman, 1987). On the other hand, r_b is the smallest of the three resistances used to determine v_d and does not usually have much influence on v_d.

The main component of the surface resistance (r_s) is the canopy resistance, r_c, which is parameterized in BDRYDEP as (Wesely, 1989):

$$r_c = r_m\{1 + [200/(S+0.1)]^2\}\{400/[T_s(40-T_s)]\} \quad (4)$$

where S = incoming solar radiation, T_s = surface temperature, and r_m = minimum r_c resistance. The parameter r_m is a vegetation related parameter provided to BDRYDEP and is determined by season and type of plant cover. However, equation (4) is used only when T_s is warmer than 0°C and cooler than 40°C. Should T_s fall outside this temperature range, then r_c is:

$$r_c = r_m\{1 + [200/(S+0.1)]^2\}\{100\} \quad (5)$$

Therefore, this temperature dependent parameterization of r_c (i.e., equations (4) and (5)) assumes that plants are most active when T_s is near 20°C, less active as T_s moves away from 20°C and relatively inactive when T_s is near or below 0°C or near or above 40°C.

This preliminary evaluation of surface uptake formulations was not performed directly

on BDRYDEP, but on an allied module, MODDEP2, which can be used for site calibrations. However, MODDEP2 parameterizes r_a, r_b, and r_c somewhat differently than equations (2), (3), (4) and (5) as described below. The consequences of the different parameterizations are addressed in the final section of this chapter: Initial Assessment of the RADM Deposition Module.

Following Hicks et al. (1985), MODDEP2 parameterizes the aerodynamic resistance as:

$$r_a = A/(u\sigma_\theta^2) \tag{6}$$

where σ_θ = standard deviation of the wind direction and A depends upon atmospheric stability. If the near-surface atmosphere is unstable, A = 9, and A = 4 if it is either neutral or stable. The module assumes that these data are measured at a height of 10.0 m above the surface. MODDEP2 also provides a simple method for distinguishing unstable, stable, and neutral atmospheric conditions by assuming that unstable atmospheric conditions occur whenever solar radiation exceeds 100 Wm^{-2} and σ_θ exceeds a given critical value defined as $1.1/\log(10.0/z_0)$. All other conditions are assumed to be stable or neutral.

Once r_a has been computed, MODDEP2 next estimates the friction velocity, $u_* = \sqrt{u/r_a}$, and then computes r_b as:

$$r_b = 1.75(D_v/D)^{2/3}/ku_* = 4.375(D_v/D)^{2/3}(r_a/u)^{1/2} \tag{7}$$

where the ratio of molecular diffusivities, D_v/D, is provided in a DATA statement internal to MODDEP2. Here D_v = molecular diffusivity of water vapor and D = molecular diffusivity of the gaseous pollutant under consideration as discussed in Wesely (1989).

Finally, the canopy resistance in MODDEPP2 uses ambient air temperature T_a as a

surrogate for the surface temperature T_s. Otherwise BDRYDEP and MODDEP2 parameterize r_s in exactly the same way.

In addition to u, σ_θ, S, and T_a, MODDEP2 requires relative humidity (rh), the plant leaf wetness (c_w), and the precipitation (pr) as meteorological input data to estimate v_d. These last three input variables determine the presence or absence of leaf surface moisture and it is the leaf wetness that determines the model's canopy resistance not rh, or pr. In general, during the CODE observation period there was no precipitation and only a few occurrences of dew formation, therefore, the relative humidities were almost always dry by MODDEP2 standards (i.e., rh below 95%).

SENSITIVITY OF THE MODDEP2 TO INPUT DATA

Numerical results

Given u, σ_θ, S, T_a, rh, c_w and pr MODDEP2 calculates deposition velocity (v_d). The CODE grape-site data was used as input to MODDEP2 to perform a sensitivity analysis on v_d with land use category 2 (agricultural land) and season 1 (midsummer with lush vegetation). This analysis was performed for each of the input meteorological variables independently by determining the change in v_d that resulted from adding an assumed measurement error to the input variable. (The MODDEP2 reference height was changed from 10.0 m to 10.8 m to match the measurements.)

These sensitivity calculations were performed twice. First on the daylight subset of the full data set (about 26 daylight periods between 10 am and 4 pm) and second on the full

data set (about 26 diurnal cycles between July 10 and August 5). The results are in Tables 1 and 2.

TABLE 1. Sensitivity of MODDEP2 deposition velocity to input data. Daylight data set only (10 am through 4 pm), 325 data points, CODE grape site, 10 July 1991 through 5 August 1991. Average deposition velocity computed using MODDEPP2 with this data = 0.71 cm/s. Standard Deviation of deposition velocity for this data = 0.12 cm/s.

Input Variable and Assumed Measurement Error	Observed Range of Input Variable (min , max)	Sensitivity of Deposition Velocity
$u \pm 0.5$ m/s	(0.73 , 4.96)	0.127 cms^{-1}/ms^{-1}
$\sigma_\theta \pm 3.0$ deg	(6.55 , 26.1)	0.022 cms^{-1}/deg
$S \pm 20$ Wm^{-2}	(375. , 998.)	$(4.0)10^{-5}$ cms^{-1}/Wm^{-2}
$T_a \pm 5°C$	(20.2 , 35.2)	$-(1.7)10^{-2}$ $cms^{-1}/°C$
$rh \pm 5\%$	(31.7 , 67.6)	0.0
$c_w \pm 0.1$	(0.0 , 1.0)	0.0
pr	(0.0 , 0.0)	Discussed in text

TABLE 2. Sensitivity of MODDEP2 deposition velocity to input data. Full data set, 1218 data points, CODE Grape site, 10 July 1991 through 5 August 1991. Average deposition velocity computed using MODDEP2 with this data = 0.45 cm/s. Standard Deviation of deposition velocity for this data = 0.25 cm/s.

Input Variable and Assumed Measurement Error	Observed Range of Input Variable (min , max)	Sensitivity of Deposition Velocity
$u \pm 0.5$ m/s	(0.34 , 5.75)	0.071 cms^{-1}/ms^{-1}
$\sigma_\theta \pm 3.0$ deg	(0.0 , 26.1)	0.024 cms^{-1}/deg
$S \pm 20$ Wm^{-2}	(0.0 , 998.)	$(2.75)10^{-4}$ cms^{-1}/Wm^{-2}
$T_a \pm 5°C$	(12.1 , 35.4)	$-(6.35)10^{-3}$ cms^{-1}/C
$rh \pm 5\%$	(31.0 , 100.0)	$-(3.00)10^{-5}$ cms^{-1}/ %
$c_w \pm 0.1$	(0.0 , 1.0)	0.0
pr	(0.0 , 0.0)	Discussed in text

Although the results in these two tables appear straightforward, six points require discussion. First, the average deposition velocity is higher during the daylight hours than over the course of the entire day. This is because plants are more active during the day than at night, and consequently the maximum v_d occurs during the daylight hours. The standard deviation of v_d is also lower during the daylight hours because the diurnal cycle of plant behavior is not included in the daylight calculations as in the full data set.

Second, the variations in u ($\pm$ 0.5 m/s) and σ_θ ($\pm$ 3 deg), taken from Finkelstein et al. (1986), are reasonable estimates of the error that can be expected from well maintained vane and propellor type wind sensors.

Third, the deposition velocity, v_d, is more sensitive to T_a during the daylight hours than over the full diurnal cycle, again because plants are more active during the daylight hours. However, as equations (4) and (5) indicate, as T_a approaches 40°C during the day, plant activity tends to diminish. Given that high temperatures are common in the San Joaquin Valley and that the plants tend to remain active at these temperatures, the present temperature formulation of r_c in MODDEP2 and BDRYDEP may be inappropriate for the SJVAQS.

Fourth, the ambient air temperature, T_a, was measured at 9.1 m rather than at 10.8 m where u and σ_θ were measured. This slight discrepancy may somewhat bias the calculated deposition velocities. Since daytime T_a is probably slightly warmer at 9.1 m than at 10.8 m, the average v_d given in the tables is probably underestimated. This bias is unlikely to exceed 0.05 cm/s for the daylight hours (Table 1) or 0.02 cm/s for the full data set (Table 2).

Fifth, v_d is relatively insensitive to rh and c_w for the CODE meteorological conditions. However, fixing rh at 100% and c_w at 1.0 during the CODE observation period resulted in model dew formation on the leaves and a consequent reduction in the average v_d. During the daylight hours v_d = 0.48 cm/s if dew was always present and v_d = 0.34 cm/s when dew was always present for the full data set.

Sixth, rain did not occur during the CODE observation period. However, the MODDEP2 calculated v_d is sensitive to rain, but only if positive rainfall amounts are accompanied with concurrent positive values for c_w (i.e., the leaves must also be wet if it is raining). Furthermore, for the purposes of calculating v_d, MODDEP2 treats rainwater differently than dew. With the presence of rainwater on plant surfaces, MODDEP2 computed average deposition velocities that were about 8% greater than those computed when dew was always present.

Interpretation

The information in the preceeding two tables can be used in a variety of ways, but the SJVAQS needed to determine the most probable sources for introducing errors into any model determination of v_d. This is done by using the following relation:

$$\Delta v_d = \sqrt{\sum_i \left(\frac{\delta v_d}{\delta p_i}\right)^2 \Delta p_i^2} \qquad (8)$$

where Δv_d = uncertainty (or the most probable error) in v_d, Δp_i = uncertainty in the i^{th} input

variable, p_i, and $\delta v_d/\delta p_i$ = sensitivity of v_d to p_i. Using equation (8) and the results from Tables 1 and 2 the above relationship suggests that the greatest source of error in the MODDEP2 calculation for v_d is due (in almost equal amounts) to measurement errors associated with wind speed, u, and the standard deviation of the wind direction, σ_θ (both u and σ_θ affect estimates of r_a and r_b). All other meteorological inputs are of minimal importance. However, the parameterization of r_c is less certain than the parameterization of r_a and r_b. In fact, v_d is more sensitive to uncertainties in r_m than to any of the uncertainties in either r_a or r_b. However, r_m is an input parameter and can be adjusted or calibrated for different types of vegetation. In summary, the uncertainty in the modeled deposition velocity for the CODE grape data, as inferred from Tables 1 and 2 and equation (8), is estimated to be about $\pm$ 0.09 cm/s irrespective of whether the full data set or the daylight data set is used. Any differences between the observed v_d and the modeled v_d that exceed $\pm$ 0.09 cm/s indicate that the model needs some adjustment to r_s and/or r_c. The next section discusses modeled and observed deposition velocities.

INITIAL ASSESSMENT OF THE RADM DEPOSITION MODULE

The CODE grape data set also includes measurements of the ambient ozone concentration (O_3) and the ozone flux (F_{03}). Consequently, it is possible to estimate the deposition velocity directly from observations (observed $v_d = -F_{03}/O_3$). Comparing the observed v_d with the calculated v_d should provide enough information to determine whether adjustment is needed for the agricultural set of vegetation parameters as presently defined in

BDRYDEP. For the daylight-only data set the observed v_d was 0.50 cm/s $\pm$ 0.12 cm/s and for the full data set the observed v_d was 0.33 cm/s $\pm$ 0.18 cm/s. The values for v_d, as computed by the model, however, are 0.71 cm/s $\pm$ 0.12 cm/s (daylight-only, Table 1) and 0.45 cm/s $\pm$ 0.25 cm/s (full diurnal course, Table 2). The modeled deposition velocity is positively biased by about 40% relative to the observed v_d for both the daylight-only and full data sets. Because the errors introduced into the modeled v_d do not explain this difference, the vegetation parameters associated with agricultural crops need some adjustment. Changing r_m so that the modeled v_d agrees more closely to the observed v_d would accomplish this. This approach is discussed in a later chapter. This chapter discusses how the formulation of r_a and r_b in MODDEP2 influenced the calculated deposition velocites.

As shown earlier, MODDEP2 parameterizes r_a and r_b differently than does BDRYDEP. Figure 1 compares the MODDEP2 estimates of r_a with those of BDRYDEP (equation (2)), and shows that MODDEP2 also consistently and significantly overestimates r_a. Although not shown, MODDEP2 overestimates r_b by a factor of two or more. The MODDEP2 estimates of v_d are less than what would have been computed had equations (2) and (3) been used to formulate r_a and r_b. Consequently, BDRYDEP is likely to overestimate v_d by an even larger amount than does MODDEP2. In making this comparison it is important to note that the standard model estimates of r_a and r_b also contain uncertainties due to measurement-related errors just as the MODDEP2 estimate of v_d does. These measurement-related errors, derived in the appendix, are summarized as: $\Delta r_a/r_a = 0.23 \pm 0.01$ and $\Delta r_b/r_b = 0.24 \pm 0.01$. These measurement related errors are insufficient to account for the bias in the MODDEP2 parameterization scheme of r_a and r_b.

The comparison of the r_a formulations shown in figure 1, suggests that (at a minimum) a more appropriate value of A for equation (6) is needed. Other comparisons (not shown) also suggest that a new criteria for differentiating neutral and stable atmospheric conditions from unstable conditions is also required. The present criteria in MODDEP2 suggests that the critical value of σ_θ is about 17 degrees, but observations suggest that 12 degrees is more appropriate. Once these new parameterizations for r_a and r_b are completed, then the vegetation related parameters should be adjusted for the SJVAQS.

The possibility that the results of the sensitivity analysis (Tables 1 and 2) would be affected if the BDRYDEP formulations for r_a and r_b were used rather than equations (6) and (7) was tested by incorporating equation (2) directly into MODDEP2 and recalculating the sensitivities. These results indicate that BDRYDEP probably remains quite sensitive to u, but that $\delta v_d/\delta u$ is about 10% less than shown in Tables 1 and 2. (BDRYDEP is not sensitive to σ_θ because it is no longer included in the parameterization of r_a.) BDRYDEP is probably somewhat more sensitive to temperature and solar radiation than MODDEP2 and therefore, the parameterization of r_c and/or r_s is even more important for BDRYDEP than MODDEP2.

In summary, the initial assessment of BDRYDEP is that it will need a data intensive revaluation (or redetermination) of r_m and possibly a complete reparameterization of r_c and/or r_s before it can provide an accurate estimate of v_d for the SJVAQS.

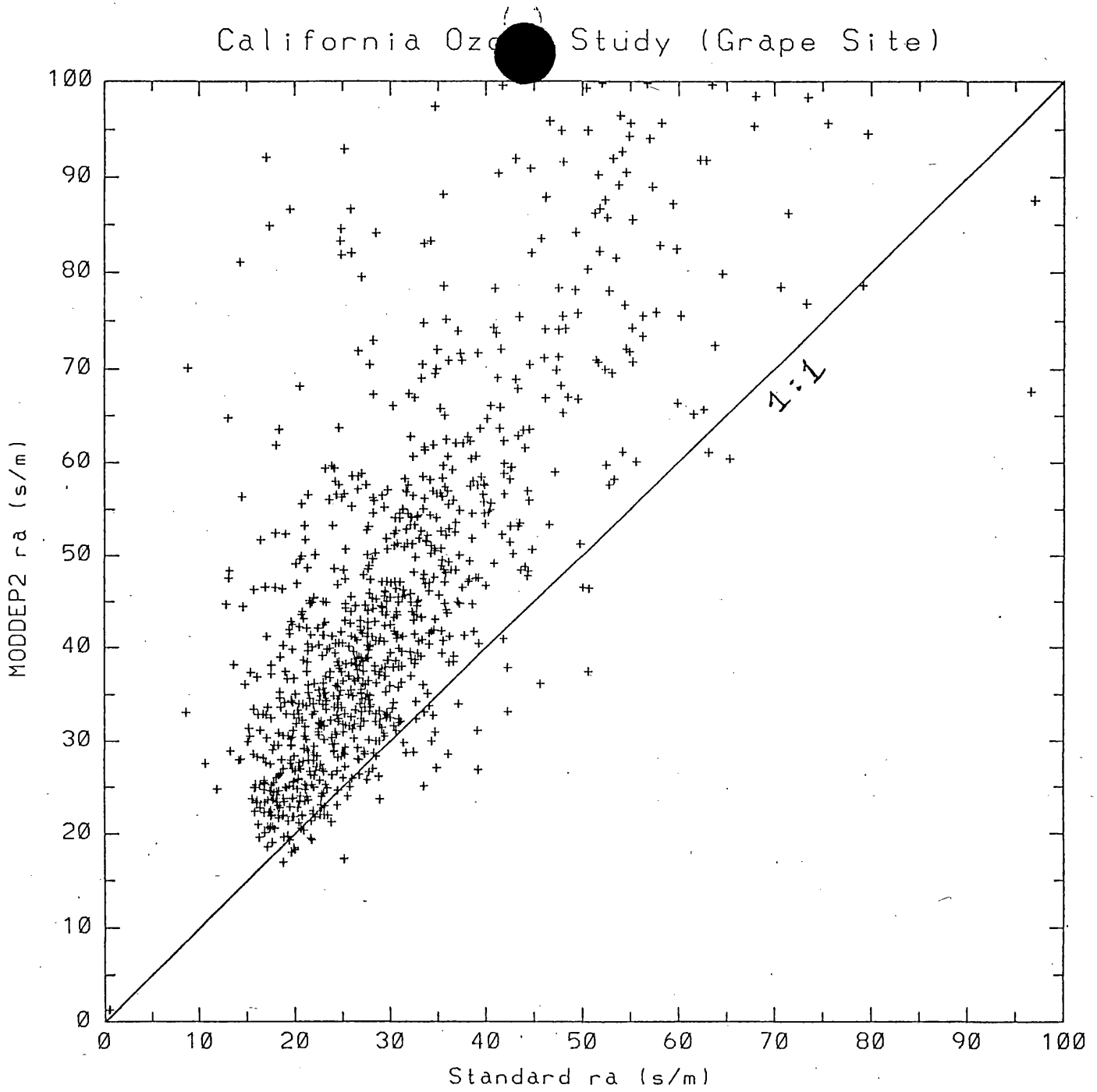
California Ozone Study (Grape Site)
MODDEP2 ra (s/m)
Standard ra (s/m)
1:1
0
10
20
30
40
50
60
70
80
90
100

REFERENCES CHAPTER I

Byun, D.W. On the analytical solutions of flux-profile relationships for the atmospheric surface layer. 1990. Journal of Applied Meteorology, 29: 652-657.

Hicks, B.B., D.D. Baldocchi, R.P. Hosker, B.A. Hutchison, D.R. Matt, R.T. McMillen, L.C. Satterfield. On the use of monitored air concentrations to infer dry deposition. 1985. NOAA Technical Memorandum ERL ARL-141, Air Resources Laboratory, Silver Springs, MD. 65 pp.

Finkelstein, P.L., J.C. Kaimal, M.E. Gaynor, M.E. Graves and T.J. Lockhart. Comparison of wind monitoring systems. Part I: In situ sensors. 1986. Journal of Atmospheric and Oceanic Technology, 3: 583-593.

Massman, W.J., Heat transfer to and from vegetated surfaces: an analytical method for the bulk exchange coefficients. 1987. Boundary-Layer Meteorology, 49: 295-397.

Wesely, M.L. Parameterization of surface resistances to gaseous dry deposition in regional-scale numerical models. 1989. Atmospheric Environment, 23: 1293-1304.

APPENDIX

Uncertainties in the resistances r_a and r_b associated with the uncertainties in the tower-based measurements

Equations (2) and (3) indicate the importance of the stability parameter, z/L, in determining r_a and r_b. Before discussing r_a and r_b it is necessary to estimate the measurement uncertainties in z/L. After some manipulation the standard formulation for z/L is:

$$z/L = -Rzkg(H + \alpha\lambda E)/C_p P u_*^3 \qquad (A1)$$

where R = universal gas constant, g = acceleration due to gravity, H = surface heat flux, and λE = surface latent heat flux, α (= 0.07) is a constant, C_p = specific heat capacity of air, and P = ambient pressure. All other symbols have been previously defined. The major uncertainties in z/L arise from the uncertainties in H, λE and u_*. A formal error analysis can be used to evaluate $\Delta(z/L)$ analytically. First, $\partial(z/L)/\partial H$, $\partial(z/L)/\partial(\lambda E)$, and $\partial(z/L)/\partial u_*$ are found from equation (A1) and then, assuming that the major measurement errors in H, λE, and u_* are independent, a method similar to that provided by equation (8) is used to derive the following expression for the uncertainty in z/L:

$$\Delta(z/L) = \sqrt{K/u_*^6 + 9(z/L)^2 \Delta u_*^2/u_*^2} \qquad (A2)$$

where $K = (Rzkg/C_pP)^2(\Delta H^2 + \alpha^2 \Delta\lambda E^2)$. To evaluate equation (A2) I assume $\Delta H = \pm$ 20 W/m^2, $\Delta\lambda E = \pm$ 20 W/m^2 and $\Delta u_*/u_* = 0.10$. However, equation (A2) shows that $\Delta(z/L)$ is dependent not only on the uncertainties in H, λE, and u_*, but also on the stability and

friction velocity. Using the CODE grape data to evaluate equation (A2) the following relation was determined: $\Delta(z/L) \leq 0.1$ for more than 50% of the observations; therefore I assume that $\Delta(z/L) = 0.1$ when estimating $\Delta r_a/r_a$ and $\Delta r_b/r_b$.

In addition to uncertainties in z/L, the measurement errors in u, z_0 and $kB_{0_3}^{-1}$ contribute to uncertainties r_a and r_b. Therefore, assuming a 10% uncertainty in z_0 and $kB_{0_3}^{-1}$ and a 20% uncertainty in u, $\Delta r_a/r_a$ and $\Delta r_b/r_b$ were evaluated by differentiating equations (2) and (3) with respect to z/L, u, z_0, and $kB_{0_3}^{-1}$ and then substituting the appropriate expressions into an equation similar to equation (8) or equation (A2). As before with z/L, the results are a function of stability. Since 80% of all observations at the grape site fall within the stability range $-0.4 < z/L < 0.4$, all the calculated $\Delta r_a/r_a$ and $\Delta r_b/r_b$ values within this range were averaged. The final result is $\Delta r_a/r_a = 23\% \pm 1\%$ and $\Delta r_b/r_b = 24\% \pm 1\%$, which was assumed representative of the relative error associated with r_a and r_b.

Chapter II

Use of a RADM-like dry deposition module for modeling the dry deposition of ozone in the San Joaquin Valley: Recommendations based on the site specific CODE91 data

PURPOSE

On the basis of the California Ozone Deposition Experiment (CODE) tower-based eddy covariance data, this chapter presents recommendations for parameterizing the surface layer uptake of ozone in the San Joaquin Valley of California. The purpose is to provide a simple and easily implemented formulation of the dry deposition of ozone to use within a larger photochemical and pollution transport model.

PRELIMINARY CONSIDERATIONS

Surface Conductance

RADM-like dry deposition modules are designed to simulate the diurnal course of the deposition velocity, v_d, for a variety of gaseous pollutants. Within most models the deposition velocity is parameterized using three resistances: aerodynamic resistance (r_a), quasi-laminar boundary layer resistance (r_b) and surface resistance (r_s). The relationship between these resistances and the deposition velocity is:

$$v_d = 1/(r_a + r_b + r_s) \quad (1)$$

The surface resistance, r_s, is usually the largest in magnitude and therefore, usually the major determinant of v_d. Without a reliable parameterization of r_s, the modeled deposition velocity can be a significant source of error. The goal of this chapter is to evaluate r_s (or for a variety of computational and biological reasons, to evaluate the inverse of r_s) for three plant covered sites in the San Joaquin Valley.

Surface conductance, g_s (= $1/r_s$), used throughout this report, is related to v_d as:

$$g_s = v_d/[1-v_d(r_a+r_b)] \quad (2)$$

To evaluate g_s at a given site the deposition velocity is estimated from the eddy covariance ozone flux data and ozone concentration data ie., ($v_d = \overline{-w'O_3'}/O_3$), where $\overline{w'O_3'}$ = observed ozone flux and O_3 = ambient ozone concentration. All ozone is assumed destroyed when it interacts with the plant and soil surfaces and the effective ozone concentration at these surfaces is zero.

Once g_s is determined from the CODE data, it can be used to test the surface resistance formulations in the RADM-like modules. In their simplest form these modules parameterize g_s as the sum of two terms. One term corresponds to the transpiring portion of the vegetation cover (g_c). A second term (g_0) corresponds to the combined effects of the nontranspiring portion of the plant cover, the soil and litter uptake and the turbulent/convective transfer beneath the canopy. Both model parameters, g_0 and g_c, vary

with plant cover or land use type.

In RADM, the transpiring canopy conductance, g_c, is modeled as a function of incoming solar radiation, S, and surface temperature, T_s, (Wesely 1989). Although it is slightly different than the original Wesely formulation for these purposes g_c is expressed as:

$$g_c = g_x[S^2/(S^2+b)][T_s(T_x-T_s)]/A \qquad (3)$$

where g_x, b, T_x and A are model parameters where g_x = maximum canopy conductance and roughly corresponds to $1/(1.6r_i)$ where r_i is the minimal canopy resistance to water vapor exchange (this depends upon plant cover or land use type). The factor of 1.6 is the ratio the molecular diffusivity of water vapor to the molecular diffusivity of ozone, T_x = maximum temperature for the plant transpiration and, because it is fixed at 40 C, is independent of plant cover type. The model parameter b is fixed at $(200\ W/m^2)^2$ and is also independent of vegetation cover type. Finally, A = $(20\ C)^2$ and, like T_x and b, is also a nonvarying model parameter. However, equation (3) is used only when T_s is between 0°C and 40°C. Should T_s fall outside this range, then the term, $T_s(T_x-T_s)/A$, is replaced by 0.01, which effectively shuts off transpiration and the plant stomatal uptake of ozone.

In RADM, g_0 is parameterized as:

$$g_0=g_1+g_2\left(\frac{S+10}{\alpha S+10\alpha+1000}\right) \qquad (4)$$

where g_1 and α are parameters determined by land use category and season, and $g_2 = 1.0$ cms $^{-1}$ is a fixed constant.

The RADM surface conductance dry deposition model evaluated in this report is:

$$g_s = g_x[S^2/(S^2+b)][T_s(T_x-T_s)]/A + g_0 \qquad (5)$$

where the parameter values g_x, b, T_x, A, g_1 and α are taken from Wesely (1989). Equations (4) and (5) together are the Wesely surface conductance model that is evaluated in this report. The land use category used in this study for the cotton and grape site corresponds to agricultural land during midsummer (land use category 2, seasonal category 1). For the grass site the land use category used in this study is represented by rangeland during the late autumn but before frost (land use category 3, seasonal category 3).

In addition to Wesely's formulation, equations (4) and (5), a simpler formulation of g_c and g_0, was also tested; it is:

$$g_s = g_x[S/(S+b)] + g_0 \qquad (6)$$

The main differences between this model and the Wesely formulation is that g_c is not a function of temperature and g_0 is not a function of solar radiation. In fact, g_0 in equation (6) is a model parameter that may vary with canopy cover type and season, but otherwise is constant. The main advantage of equation (6) over the Wesely model is that it requires fewer numerical operations to evaluate but is just as accurate in describing the cotton and

grape site data. Equation (6) may also be a more physically correct description of the bulk stomatal behavior because recent studies show that stomata of several plant species do not respond to temperature under normal environmental conditions (Massman and Kaufmann 1991; and Massman 1992).

Aerodynamic and quasi-laminar boundary layer resistances

The aerodynamic and quasi-laminar boundary layer resistances with equation (2) used in the present analysis are:

$$r_a = [\log(\{z-d\}/z_0) - \psi_m(z/L)][\log(\{z-d\}/z_0) - \psi_c(z/L)]/k^2u \quad (7)$$

$$r_b = kB_{0_3}^{-1}[\log(\{z-d\}/z_0) - \psi_m(z/L)]/k^2u \quad (8)$$

where z = the height above the ground surface at which the measurements are made, k (=0.4) is the von Karman constant, L = the Obukhov length, z_0 = surface roughness length, d = surface displacement height, u = horizontal wind speed, $kB_{0_3}^{-1}$, defined below by equation (9) is a vegetation/pollutant related parameter adapted from Massman (1987) and ψ_m and ψ_c, the Businger-Dyer stability functions (Paulson 1970; Businger et al. 1971), are defined by equations (10) and (11) below.

$$kB_{0_3}^{-1} = 2.1u_*^{1/4} \quad (9)$$

$$\psi_m(z/L) = \begin{cases} 2\ln[(1+x)/2]+\ln[(1+x^2)/2]-2\tan^{-1}x+\pi/2 & z/L \le 0 \\ -5z/L & z/L \ge 0 \end{cases} \quad (10)$$

$$\psi_c(z/L) = \begin{cases} 2\ln[(1+x^2)/2] & z/L \le 0 \\ -5z/L & z/L \ge 0 \end{cases} \quad (11)$$

Here $x = (1 - 16z/L)^{1/4}$. These stability functions essentially follow Brutsaert's (1984) approach, except that they apply even when $1 \le z/L$. In evaluating z_0 and d the following relationships are used: $z_0 = h/8$ and $d = 2h/3$, where h is the canopy height and is a measured quantity.

In a site specific context, equations (7) and (8) are thought to provide appropriate formulations for r_a and r_b. However, several factors can introduce significant errors into any estimates of r_a and r_b based on these equations. The last chapter suggested that inherent measurement errors could cause about a 25% error in the estimates of r_a and r_b. There are other formulations for r_a and r_b that could have been used in place of equations (9), (10), and (11). For example, estimates of r_a and r_b derived with the stability formulation of Carl et al. (1973) or Wesely and Hicks (1977) differed from the present ones by about 5%. Although, the Wesely and Hicks (1977) formulation for kB_{03}^{-1} yielded estimates of r_b that are about 30% greater than those obtained with equation (9) and using a kB_{03}^{-1} formulation based on the results of Kustas et al. (1989) yields even larger estimates of r_b. However, large

uncertainties in kB_{03}^{-1} and/or r_b usually do not result in large uncertainties in g_x or g_0 because r_b is usually small compared to r_a. Finally, many site specific studies have demonstrated the existence and importance of a roughness sublayer just above plant canopies (see Cellier and Brunet 1992 for a discussion). The presence of this highly turbulent region, which was not taken into account in equations (7) and (8), tends to reduce r_a and r_b below predictions from these two equations (Garratt 1980). As discussed later in this report, some adjustment for the roughness sublayer will be made at the cotton site. All of these uncertainties contribute to uncertainties in g_s (and/or g_x and g_0). This problem is also addressed later in this report.

In addition to the various formulations of r_a and r_b discussed above, there is at least one other important formulation to discuss. In the preceding report, the MODDEP2 formulation of r_a and r_b appeared to overestimate the r_a and r_b values determined from equations (7) and (8), suggesting some recalibration of the MODDEP2 formulation would be required. The details of this recalibration are in the first appendix.

Flux corrections necessary at the cotton site

The half-hour fluxes of ozone, water vapor and carbon dioxide at the cotton site do not include some important corrections. (However, such corrections were applied when creating the half-hour flux files from the grape and grass sites.) Therefore, the cotton site data require the application of these corrections before analysis. In this report all cotton site H_2O and CO_2 fluxes have had the Webb-Pearman-Leuning correction applied. The water vapor flux data have had the oxygen correction applied; the ozone data have had the water

vapor correction applied; and the carbon dioxide data include a gain of 0.42 recommended by the designer of the instrument. The details concerning these corrections and all other matters discussed in this chapter are given in appendix II, which is a listing of the computer code developed for the analysis of the CODE data.

Flux corrections arising from sensor geometry and design

Following Moore (1986), algorithms, were developed to correct the fluxes of heat, water vapor, ozone, and carbon dioxide for relative sensor placement, sensor line averaging effects and sensor response time. Sometimes the corrections were functions of wind speed and stability, sometimes not. The specific algorithms are in Appendix II. Table 1 is a summary of the maximum values of the corrections used for each site. Table 1 provides estimates for the momentum flux correction. Although this correction was not made to the observed Reynolds' stresses, the momentum correction was used to determine if all corrections when taken together had any influence on the value of the stability parameter (z/L). The results indicated that the stability parameter did not need any adjustment since the correction factor was only about 2% for any site and any stability.

TABLE 1

Maximum flux loss corrections from sensor geometry and design

	Cotton		Grape		Grass	
	stable	unstable	stable	unstable	stable	unstable
Heat	9%	2%	3%	1%	10%	2%
O_3	11%	3%	15%	4%	28%	8%
H_2O	8%	2%	11%	3%	26.5%	8%
CO_2	16%	3%	15%	4%	26.5%	8%
Momentum	4%	3%	15%	4%	*	*

* The UCD 3-axis sonic data did not include a correction for shadowing. Since this correction may exceed the correction associated with sonic geometry, no correction was estimated.

As indicated, fluxes require larger corrections when the near-surface conditions are stable than when unstable. Therefore, the daytime fluxes that account for most of the exchange between the surface layer and the atmosphere need relatively small corrections.

Roughness sublayer

Although a roughness sublayer has been observed under unstable atmospheric conditions over a wide variety of canopies, the depth of the roughness sublayer varies with canopy geometry and is usually confined to a few meters just above the canopy. To insure the best possible estimate of g_s, the CODE data was tested for the presence of the roughness sublayer with the intent of adjusting r_a and r_b if necessary.

The influence of the roughness was determined by comparing the observed friction velocity u_{*obs} with the friction velocity (u_{*calc}) calculated as a solution to the following:

$$u = u_{*calc}/k[f_1 - \psi_m(f_2/u^3_{*calc})] \qquad (12)$$

where $f_1 = \log(\{z-d\}/z_0)$ and $f_2 = -kgz(\overline{w'T'}+0.61T\overline{w'\rho_v'}/\rho_a)/T$ and g = acceleration due to gravity, $\overline{w'T'}$ = heat flux, $\overline{w'\rho_v'}$ = water vapor flux, ρ_a = ambient atmospheric density, and T = ambient temperature. Equation (12) is the standard formulation for relating horizontal wind and friction velocity. If any measurements are being made that are sufficiently close to the roughness sublayer generally, $u_{*obs} > u_{*calc}$ (i.e., the height at which the data are taken is more turbulent than the standard flux gradient relationship would indicate). This idea is implemented by determining the regression coefficient, a, in the following equation: $u_{*obs} = au_{*calc}$. Table 2 gives the values of a with the standard error of the estimate (SEE) and the

number of data points (N) used to determine them. All values with $u_{*obs} > 4u_{*calc}$ were excluded from this test. Furthermore, all values of $|z/L| > 2.0$ at the grape and cotton sites, and $|z/L| > 8.0$ at the grassland site were excluded from this test and from calculations performed for this chapter.

TABLE 2

Regression coefficients testing for overt presence of the roughness sublayer

	Cotton		Grape		Grass	
	stable	unstable	stable	unstable	stable	unstable
a	0.966	1.163	1.010	0.986	1.012	0.951
SEE	0.018	0.019	0.006	0.007	0.009	0.008
N	446	530	666	466	311	449

Table 2 demonstrates that the cotton data are probably strongly affected by the roughness sublayer during unstable atmospheric conditions. Although there is little reason to explicitly account for the roughness sublayer at any other stability or site, this test should not be misconstrued as indicating a lack of a roughness sublayer at either the grape or grass sites. All that can be concluded is that the height above the surface at which the measurements are made is well removed from the roughness sublayer at these other two sites. As a consequence of these results, all calculations of r_a and r_b at the cotton site are reduced by 15% to compensate for the roughness sublayer effects. This reduction is also applied to the stable conditions to avoid introducing a discontinuity in the calculations of r_a

and r_b at neutral conditions.

Because this simple semi-empirical method for correcting r_a and r_b does not eliminate inherent uncertainties it is necessary to evaluate the sensitivity of the model parameters to uncertainties in r_a and r_b.

RESULTS

The first three figures show the data-derived g_s as a function of time of the day for the cotton (fig. 1), the grape (fig. 2), and the grass (fig. 3) sites. For the two agricultural sites (cotton and grape), a few outliers were removed from the basic data set. At the grape site at least half of these outliers were associated with some moisture on the leaves (as was indicated by a positive reading of the leaf wetness sensors) and virtually all outliers at both sites occurred during the nighttime hours or early in the morning and were usually much larger than anything shown in figures 1 or 2.

At the cotton and grape sites, the diurnal course of the canopy conductance is clearly evidenced. At the grass site, however, the plant stomatal activity is nearly nonexistent because the plants have largely ceased transpiring. Comparing the surface conductance for cotton and grape canopies also indicates that the ozone uptake by cotton is approximately two to three times that of grape, which is in good quantitative agreement with the leaf-level CO_2 and water vapor exchange measurements made by David Grantz at these same sites. The difference in ozone uptake between these two crops is quite significant, particularly in relation to any modeling efforts. The difference indicates that it may be necessary to define

species-level land use categories rather than lump all agricultural crops into one category.

Figures 4, 5 and 6 compare the data-derived g_s with the Wesely version of g_s for the three CODE sites. In all three cases the Wesely g_s overestimates the observed g_s; however, the Wesely g_s is not severely biased for cotton and may be acceptable for modeling application in the San Joaquin Valley. A considerably better fit to these data is possible with the Wesely g_s model (equations 4 and 5) by optimizing on the parameters g_x and g_1. Table 3 lists the original and optimized values of the model parameters and the standard error of the estimate (SEE) for the model fit to the data for each set of parameter values.

TABLE 3

Quality of the modeled g_s for the Wesely model. The units associated with all numerical values are cm/s.

	Cotton			Grape			Grass		
	g_x	g_1	SEE	g_x	g_1	SEE	g_x	g_1	SEE
original	1.00	0.34	0.36	1.00	0.34	0.36	0.00	0.34	0.32
optimized	1.04	0.20	0.34	0.36	0.21	0.15	0.00	0.05	0.02

The bias in the original formulation is indicated by the differences between the optimized and original values of g_x and g_1. Clearly g_1 shows a positive bias over all these canopies. However, although the original value for g_x is probably biased for grapes, it is not significantly biased for cotton.

Table 4 is the same as table 3 except that the model used for g_s is equation (6).

TABLE 4

Quality of the proposed simpler model for g_s, i.e., equation (6). The units associated with all numerical values are cm/s. The parameter b was fixed at 3300 W/m^2 for cotton and grape.

Cotton			Grape			Grass		
g_x	g_0	SEE	g_x	g_0	SEE	g_x	g_0	SEE
5.13	0.22	0.26	1.91	0.22	0.14	0.00	0.14	0.14

Comparing the SEE values for g_s shown in tables 3 and 4, the model represented by equation (6) is slightly better than the optimized version of the Wesely model for describing the grape and grass data but is significantly better for describing the cotton data. Equation (6) with the parameter values shown in table 4 accounts for 77% of the variance of the data-derived g_s values for cotton (fig. 1) and 59% of the variance of the grape data (fig. 2). It is important to note here that the optimized version of the Wesely model accounted for 60% of the variance of the cotton data and 56% of the variance of the grape data, while the unoptimized version of the Wesely model accounted for 55% of the variance of the cotton data.

Table 5 gives the standard error estimate of g_x for the g_x values shown in table 4 and includes the uncertainty in g_x estimated from the sensitivity analysis performed by varying r_a

and r_b.

TABLE 5

Standard error of the estimate for g_x (cotton and grape) and g_0 (grass) listed in table 4 and uncertainties resulting from a simultaneous (and arbitrary) 50% change in r_a and r_b. The units associated with all numerical values are cm/s. For cotton and grape the parameter b was fixed at 3300 W/m^2 and the parameter g_0 was fixed at 0.22 cm/s. For grass the parameter g_x was fixed at 0.0 cm/s.

	Cotton	Grape	Grass
SEE	0.09	0.04	0.008
Uncertainty	$>1.34^*$	0.40	0.009

* For a 50% decrease in r_a and r_b, g_x was reduced by 1.34 cm s^{-1}; whereas g_x increased by 8.49 cm s^{-1} when r_a and r_b were increased by 50%.

The uncertainty in g_x associated with an uncertainty in r_a and r_b is always a significant fraction (e.g., at least 20% for the agricultural crops) of g_x. This suggests that any modeling of ozone uptake by the surface based on the CODE data is probably uncertain to at least 20%, and may have an even greater percentage uncertainty.

Table 5 also shows that the cotton canopy is more sensitive to uncertainties in r_a and r_b than the grape canopy. This is because the canopy resistance for cotton is, as Table 4 and

Figures 1 and 2 indicate, at least a factor of 2 smaller than the grape canopy resistance. In fact, the canopy resistance for cotton is so low that it typically is only a factor of 2 greater than r_a and r_b; whereas, for grape the canopy resistance is almost a factor of 10 greater than r_a and r_b. Since the cotton canopy resistance is so low when compared with r_a and r_b, it is more sensitive to changes in r_a and r_b than the grape canopy. This is particularly true when r_a and r_b are increased and the canopy resistance is decreased to be consistent with the observed deposition velocities. A similar sensitivity analysis was performed with the Wesely model and the results are similar to those shown in Table 5 and discussed above.

RECOMMENDATIONS

Based on the preceding results at least two alternative recommendations can be made. The first recommendation is to optimize the present RADM-like surface parameterization module as per Table 3. That is increase the minimum stomatal resistance (denoted by Wesely (1989) as r_i) by 50% for agricultural land during midsummer. Increase all other resistances, within the agricultural land use and midsummer seasonal categories which define g_0 (denoted by Wesely (1989) as r_{lu}, r_{ac}, r_{dc}, r_{gs0}, and r_{c10}) by 67%. Maintain the same value of r_i for the late autumn and grassland categories, but increase all resistances that define g_0 for the late autumn and grassland categories by 500 to 600%. No recommendations concerning other land use or seasonal categories are possible with the present data set. This approach, simply adjusting the current model for the San Joaquin Valley, although useful as an initial calibration point for further studies, does not consider important phenological

differences between plant species located throughout the valley, and does not address the area representativeness of the plant cover.

A second, more radical recommendation, follows. If the data used to drive RADM includes surface temperatures near or above 40°C, then the recommendations above for adjusting the Wesely model will be useless. This is because the Wesely model effectively stops transpiration and plant uptake of ozone at 40°C. Consequently, the canopy parameterization scheme should be completely redone using equation (6) and parameter values g_x, g_0, and b should be chosen in accordance with the values in table 4. To reformulate the Wesely surface model: (1) remove all terms associated with g_2 [equation (4)] of the Wesely model; (2) replace all terms relating to equation (3) with $g_x[S/(S+b)]$ (here $b=3300$ Wm^{-2}); (3) increase all resistances associated with g_0 by 50% for agricultural crops during midsummer and by 150% for late autumn grasslands; (4) decrease r_i by 50% for grapes or 80% for cotton.

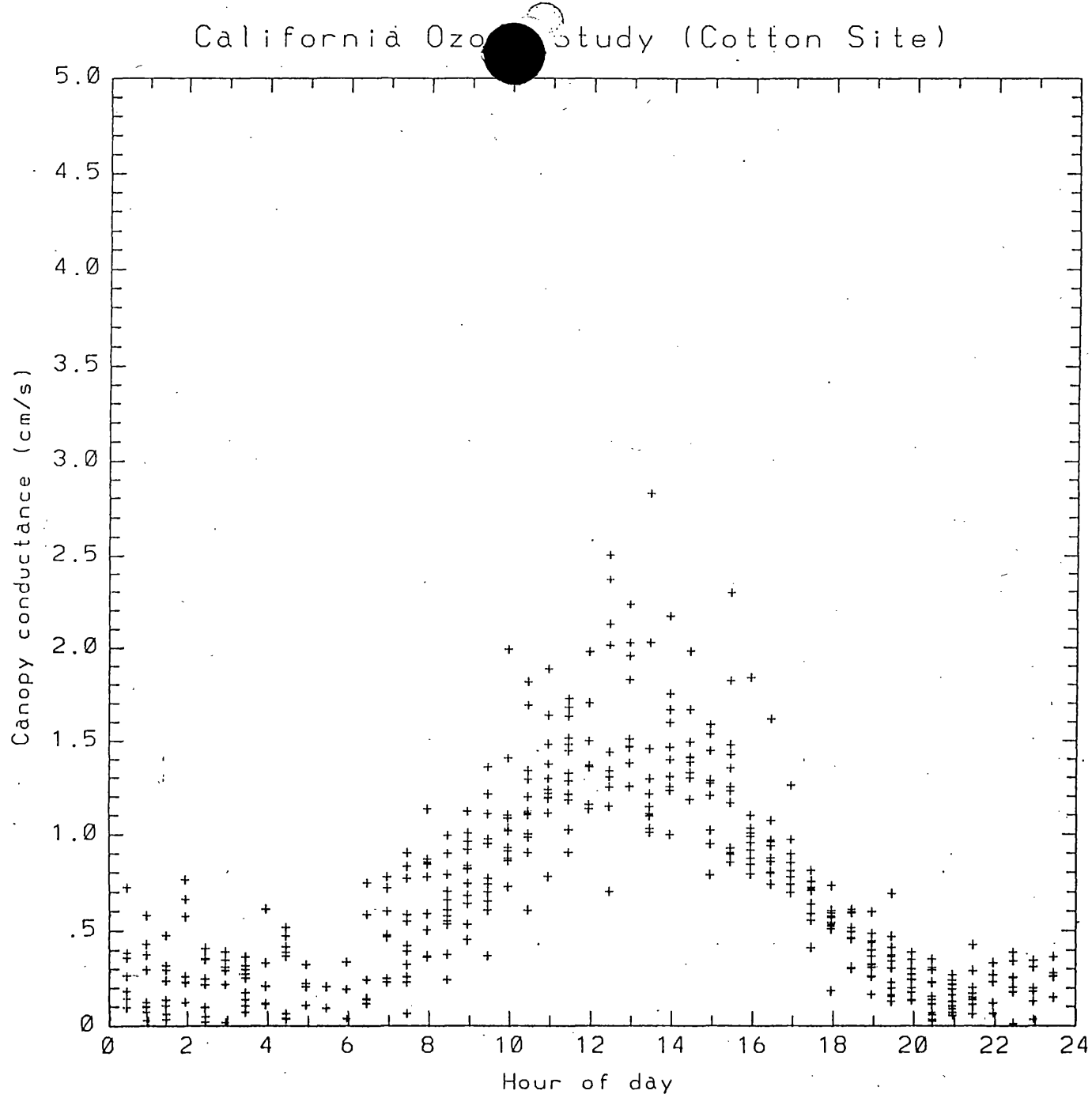
California Ozone Study (Cotton Site)
Canopy conductance (cm/s)
5.0
4.5
4.0
3.5
3.0
2.5
2.0
1.5
1.0
.5
0
0
2
4
6
8
10
12
14
16
18
20
22
24
Hour of day

Fig. 4

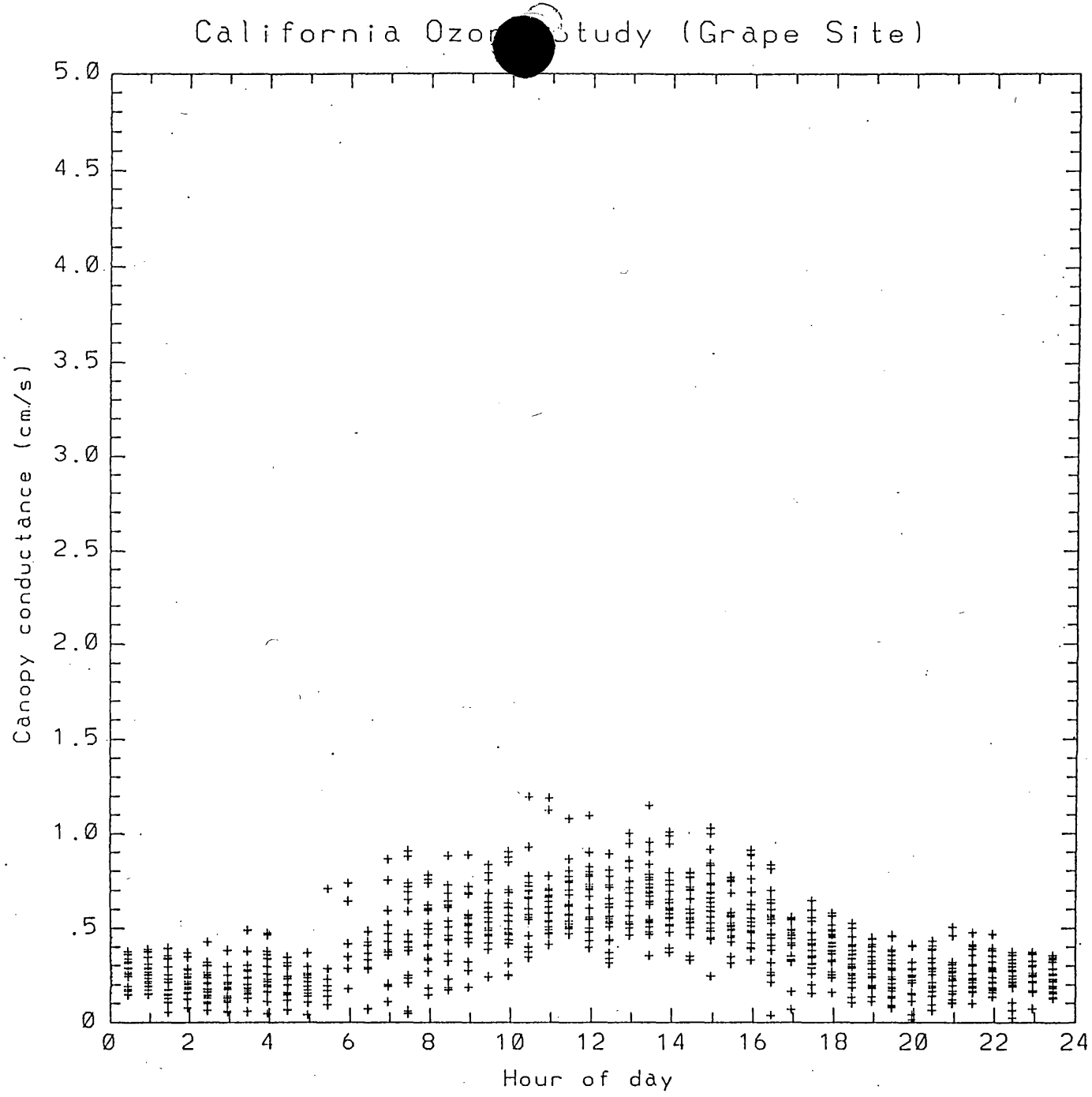
California Ozone Study (Grape Site)
Canopy conductance (cm/s)
5.0
4.5
4.0
3.5
3.0
2.5
2.0
1.5
1.0
.5
0
0
2
4
6
8
10
12
14
16
18
20
22
24
Hour of day

Fig. 2

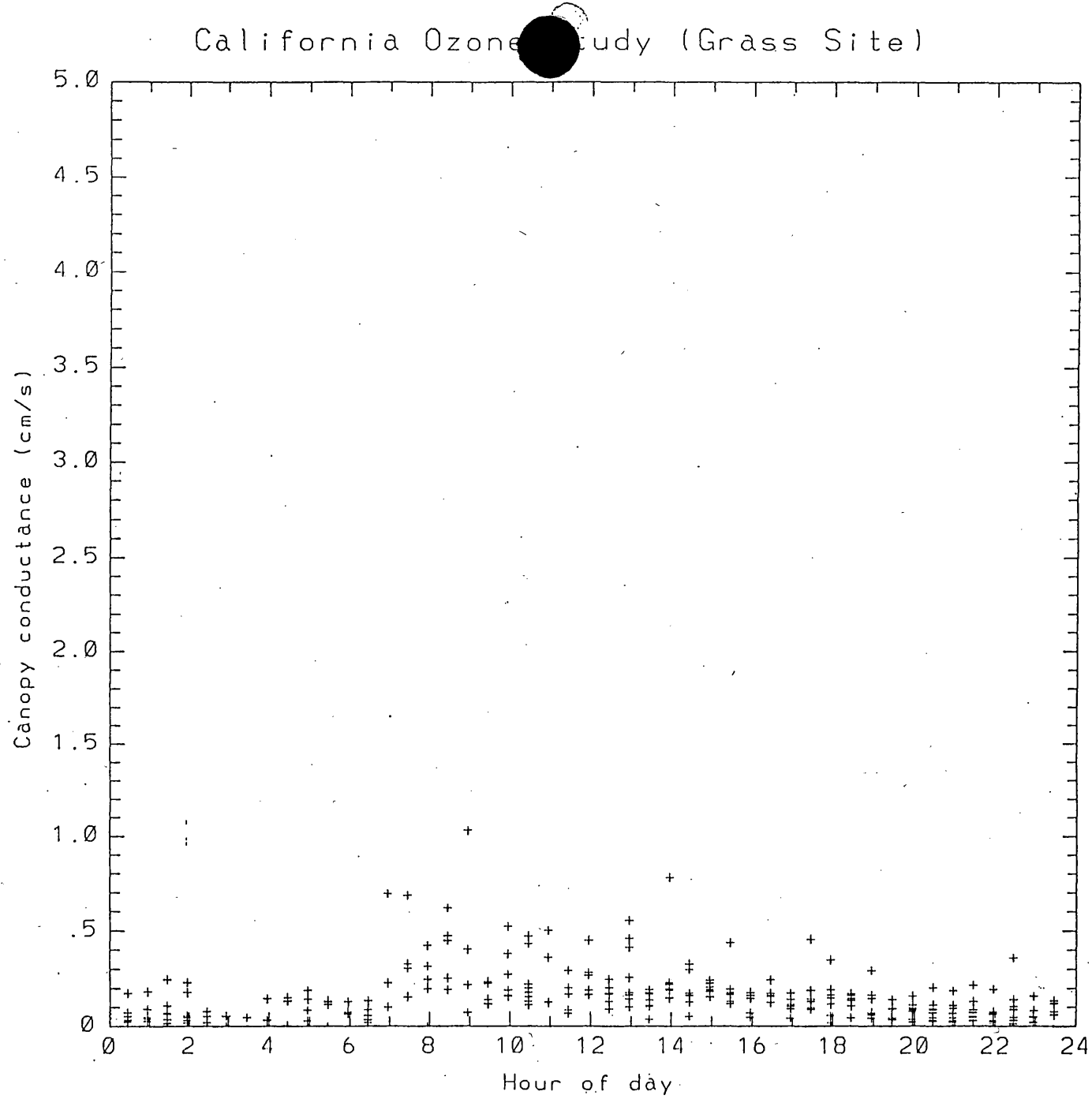
California Ozone Study (Grass Site)
Canopy conductance (cm/s)
5.0
4.5
4.0
3.5
3.0
2.5
2.0
1.5
1.0
.5
0
0
2
4
6
8
10
12
14
16
18
20
22
24
Hour of day

Fig. 3

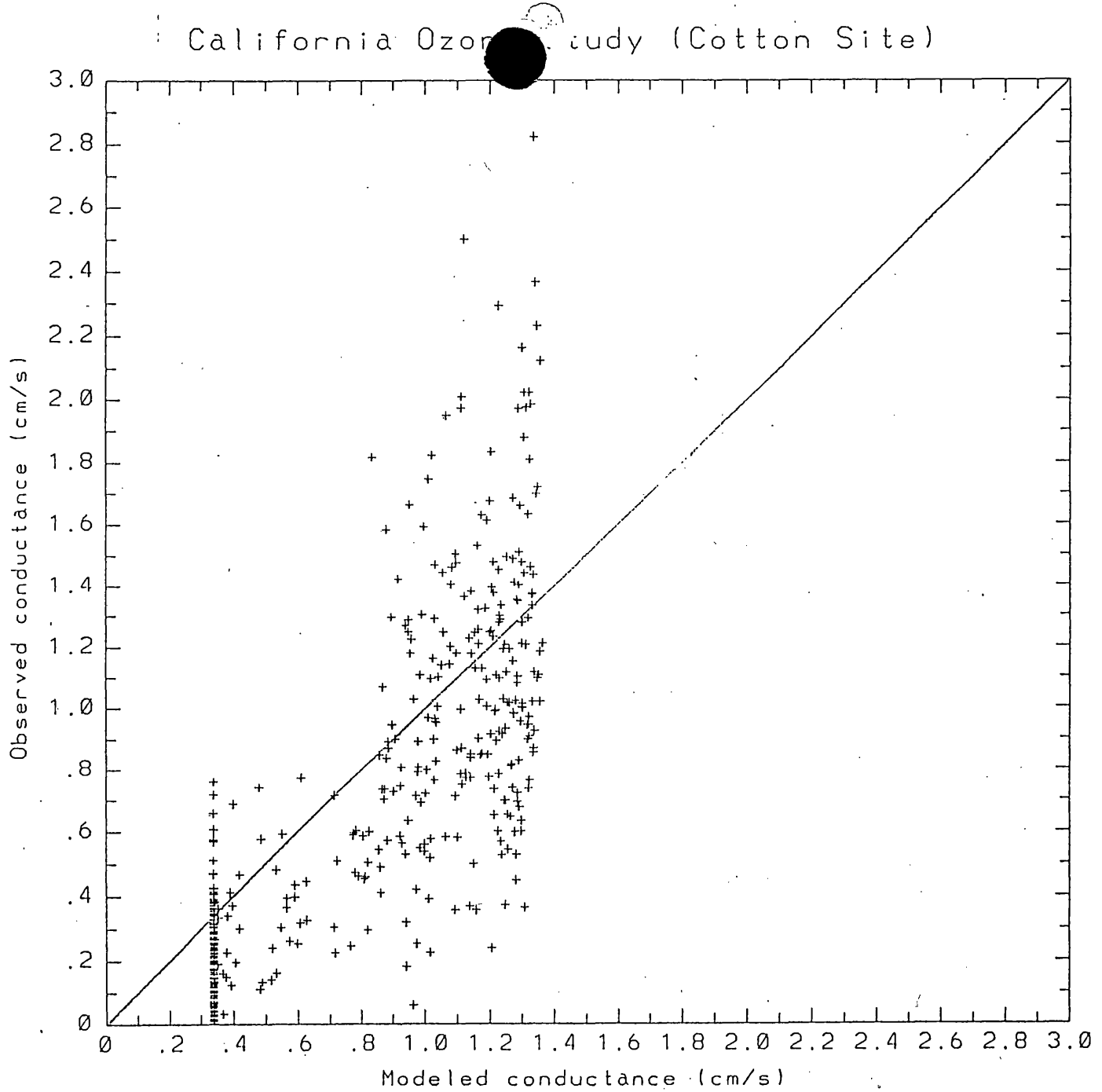
California Ozon udy (Cotton Site)
Observed conductance (cm/s)
Modeled conductance (cm/s)
0
.2
.4
.6
.8
1.0
1.2
1.4
1.6
1.8
2.0
2.2
2.4
2.6
2.8
3.0

Fig. 4

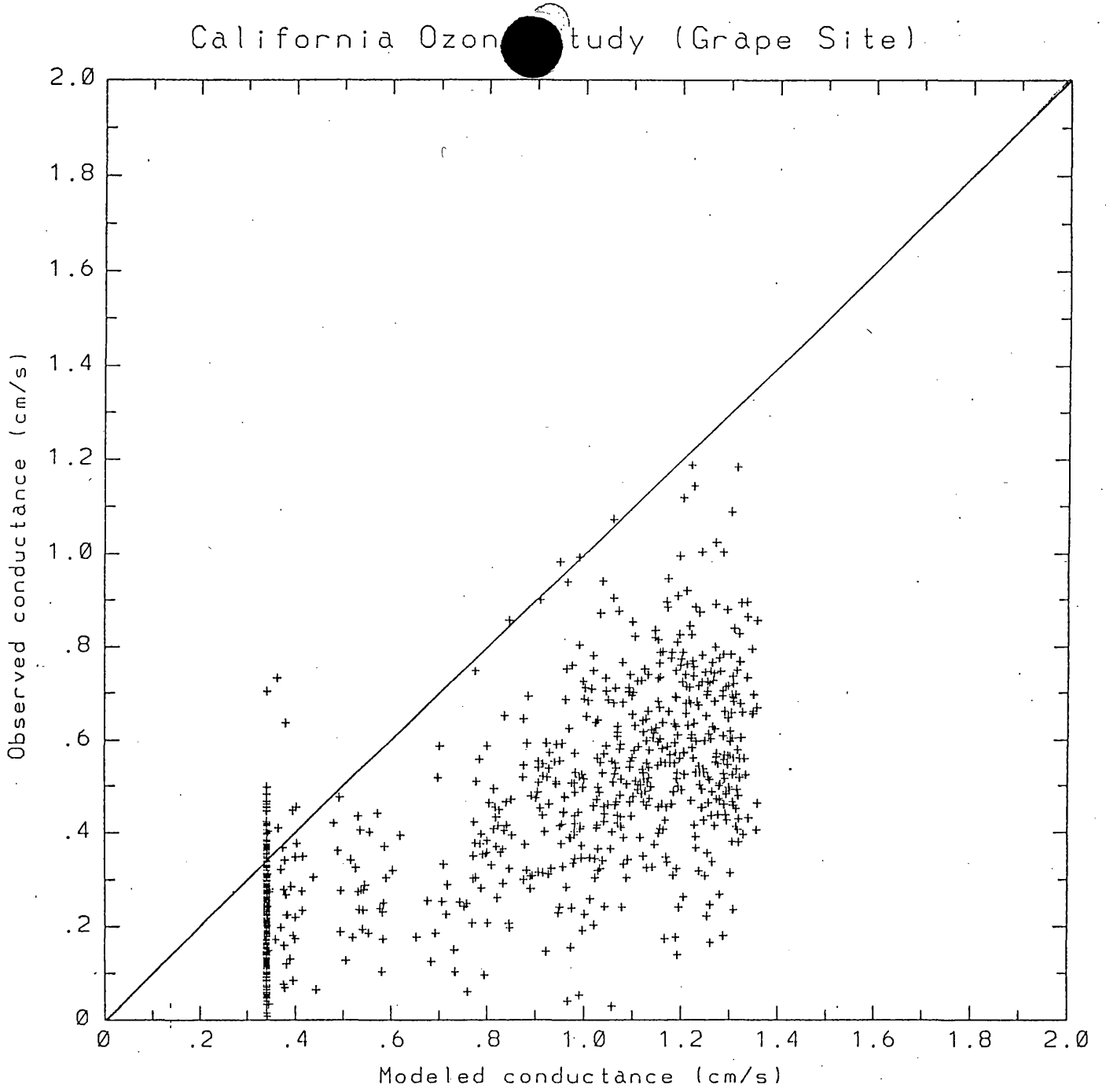
California Ozon tudy (Grape Site)
Observed conductance (cm/s)
Modeled conductance (cm/s)
0
.2
.4
.6
.8
1.0
1.2
1.4
1.6
1.8
2.0

Fig. 5

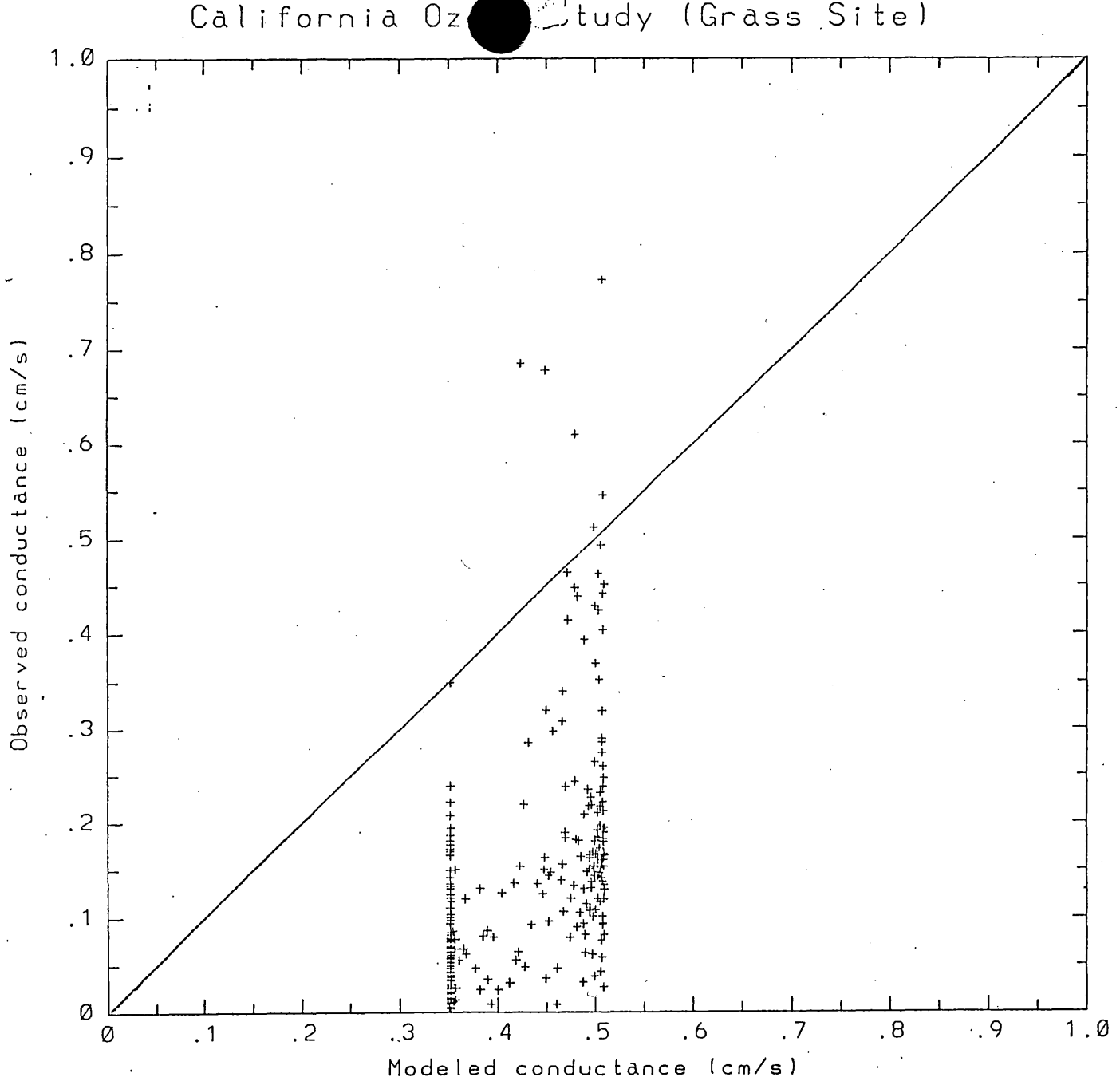
California Oz tudy (Grass Site)
Observed conductance (cm/s)
Modeled conductance (cm/s)
1.0
.9
.8
.7
.6
.5
.4
.3
.2
.1
0
0
.1
.2
.3
.4
.5
.6
.7
.8
.9
1.0

Fig.6

REFERENCES CHAPTER II

Brutsaert, W. *Evaporation into the atmosphere.* 1984. D. Reidel, Dordrecht, pp. 299.

Businger, J.A., J.C. Wyngaard, Y. Izumi and E.F. Bradley. Flux-profile relationships in the atmospheric surface layer. 1971. Journal of the Atmospheric Science, 28: 181-189.

Carl, D.M., T.C. Tarbell and H.A. Panofsky. Profiles of wind and temperature from towers over homogeneous terrain. 1973. Journal of the Atmospheric Science, 30: 788-794.

Cellier, P. and Y. Brunet. Flux-gradient relationships above tall plant canopies. 1992. Agricultural and Forest Meteorology, 58: 93-117.

Garratt, J.R. Surface influence upon vertical profiles in the atmospheric near-surface layer. 1980. Quarterly Journal of the Royal Meteorological Society, 106: 803-819.

Kustas, W.P., B.J. Choudhury, M.S. Moran, R.J. Reginato, R.D. Jackson, L.W. Gay and H.L. Weaver. Determinations of sensible heat flux over sparse canopy using thermal infrared data. 1989. Agricultural and Forest Meteorology, 44: 197-216.

Massman, W.J. Heat transfer to and from vegetated surfaces: an analytical method for the bulk exchange coefficients. 1987. Boundary-Layer Meteorology, 49: 269-281.

Massman, W.J. A surface energy balance method for partitioning evapotranspiration data into plant and soil components for a surface with partial canopy cover. 1992. Water Resources Research, 28: 1723-1732.

Massman, W.J. and M.R. Kaufmann, Stomatal response to certain environmental factors: a comparison of models for subalpine trees in the Rocky Mountains. 1991. Agricultural and Forest Meteorology, 54: 153-167.

Moore, C.J. Frequency response corrections for eddy correlation systems. 1986. Boundary-Layer Meteorology, 37: 17-35.

Paulson, C.A. The mathematical representation of wind and temperature profiles in the unstable atmospheric surface layer. 1970. Journal of Applied Meteorology, 9: 857-861.

Wesely, M.L. Parameterization of surface resistances to gaseous dry deposition in regional-scale numerical models. 1989. Atmospheric Environment, 23: 1293-1304.

Wesely, M.L. and B.B. Hicks. Some factors that affect the deposition rates of sulphur dioxide and similar gases on vegetation. 1977. Journal of the Air Pollution Control Association, 27: 1110-1116.

APPENDIX I

A recalibration of the MODDEP2 formulation for r_a and r_b

In the previous report to the California Air Resources Board, the need to recalibrate the formulation of r_a and r_b was outlined. This appendix presents the results of that recalibration.

MODDEP2 estimates r_a using the following relationship:

$$r_a = C_v^2/u\sigma_\theta^2 \qquad (I.1)$$

where C_v = constant coefficient (equal to 3 for unstable atmospheric conditions and 2 for stable conditions) and σ_θ = standard deviation of the wind direction. MODDEP2 provides a simple method for distinguishing between unstable and stable or neutral atmospheric conditions. The formulation assumes that unstable atmospheric conditions occur whenever solar radiation exceeds 100 W/m^2 and σ_θ exceeds a critical value defined as $1.1/\log(z_{ref}/z_0)$, where z_{ref} is the measurement height of u and σ_θ. All other conditions are assumed to be stable or neutral. Once r_a has been computed, MODDEP2 estimates r_b (after some simplification) as: $r_b = 6(r_a/u)^{1/2}$. Any errors in r_a probably are in r_b which is what was found and is discussed in the previous report. The reason that r_a and r_b are overestimated by the MODDEP2 approach is that the coefficient C_v is overestimated. Using equation (6) of the main text, the Businger definition for r_a, C_v was found by regression for the three CODE

sites. The results of the regression are in the following table.

TABLE I.1

C_v values, their standard error of the estimate, σC_v, and the number of data points used in the regression (N).

	Cotton			Grape			Grass		
	C_v	σC_v	N	C_v	σC_v	N	C_v	σC_v	N
$2.0 > z/L > 0.02$ STABLE	1.49	(0.03)	362	1.66	(0.01)	629	2.55	(0.08)	250
$-0.02 < z/L < 0.02$ NEUTRAL	1.88	(0.07)	212	1.73	(0.04)	50	2.28	(0.09)	87
$-2.0 < z/L < -0.02$ UNSTABLE	1.89	(0.03)	453	1.61	(0.02)	435	3.29	(0.05)	340

The first row of this table corresponds to stable conditions, the results for neutral condition are the second row, and results appropriate to unstable conditions are the third row. C_v is always less than what MODDEP2 assumes and a more appropriate value for the critical value of σ_θ is $0.75/\log(z_{ref}/z_0)$ rather than the $1.1/\log(z_{ref}/z_0)$ used by MODDEP2. These present results suggest a more suitable value for C_v^2 for agricultural crops in equation

(I.1) is 3.0 and that no distinction be made for atmospheric stability. However, the C_v^2 value for the grassland site is somewhat larger than that used in MODDEP2 and does show some stability dependency. The results in Table I.1 suggest that the architecture of the plant canopy may be more important to the value of the transfer coefficient, C_v, than atmospheric stability.

APPENDIX II

A listing of the computer code (CALIF1.F77) used in the analysis

This appendix details the methods of analysis used to examine the ozone deposition data taken at the three tower-based CODE sites. Although not discussed in this report, this program is also used to investigate evapotranspiration and CO_2 exchange and other processes important to atmosphere-surface interactions. The fortran 77 program, CALIF1, has been successfully executed many times on the Forest Service's DG 20000 computer system and is available from the author upon request.

APPENDIX III

TO: Jim Pederson, Julius Chang and Phil Roth

FROM: Bill Massman (4-12--93)

SUBJECT: Recommended changes to BDRYDEP (the surface formulation for Ozone uptake used in RADM) from CODE91 data analysis.

Based on the analysis of the CODE data completed in January 1993, I recommended the following changes be made to BDRYDEP.

(1) Remove from the RDC and RDCL terms of the computer code the following term:

100.*(1.+1000./(RADIAT(J)+10.))

This eliminates the convective turbulent transfer to the lower portion of the canopy.

(2) Assign a value of 1.0 to TTRM1 of the computer code.

This eliminates the stomatal temperature dependency.

(3) Rewrite the computer code as follows:

RTRM = 3300./(RADIAT(J) + 0.0001)

RIO(J) = RI(...)*WET(1.0 + RTRM)

This change makes the computer code consistent with the new model (Massman, DRAFT INTERIM REPORT to CARB, "On the use of RADM-like dry deposition module for modeling the dry deposition of ozone in the San Joaquin Valley: recommendations based on the site specific CODE91 data") for canopy uptake of

ozone. This change also implicitly scales the canopy uptake of all other pollutants to ozone uptake as discussed in Wesely (1986, Atmos. Environ., 23, 1293-1304.)

(4) Increase all resistance associated with g_0 (i.e., r_{lu}, r_{ac}, r_{dc}, r_{gs0}, and r_{c10}) by 50% for agriculture land use during midsummer and by 150% for grasslands during late autumn. The late autumn seasonal category should be used with grasslands during July and August because the grasses are senescent during these months in the San Joaquin Valley.

(5) Decrease r_i by 50% for grapes and 80% for cotton or an overall decrease of 67% for agricultural land use.

Points (4)-(5) in effect provide the calibration for the new model of surface ozone uptake as determined from CODE91 data.

Chapter III

JOURNAL OF GEOPHYSICAL RESEARCH, VOL. 99, NO. D4, PAGES 8281–8294, APRIL 20, 1994

An evaluation of the regional acid deposition model surface module for ozone uptake at three sites in the San Joaquin Valley of California

W. J. Massman,[1] J. Pederson,[2] A. Delany,[3] D. Grantz,[4] G. den Hartog,[5] H. H. Neumann,[5] S. P. Oncley,[3] R. Pearson, Jr.,[6] R. H. Shaw[7]

Abstract. Plants and soils act as major sinks for the destruction of tropospheric ozone, especially during daylight hours when plant stomata open and are thought to provide the dominant pathway for the uptake of ozone. The present study, part of the California Ozone Deposition Experiment, compares predictions of the regional acid deposition model ozone surface conductance module with surface conductance data derived from eddy covariance measurements of ozone flux taken at a grape, a cotton, and a grassland site in the San Joaquin Valley of California during the summer of 1991. Results indicate that the model (which was developed to provide long-term large-area estimates for the eastern United States) significantly overpredicts the surface conductance at all times of the day for at least two important types of plant cover of the San Joaquin Valley and that it incorrectly partitions the ozone flux between transpiring and nontranspiring components of the surface at the third site. Consequently, the model either overpredicts or inaccurately represents the observed deposition velocities. Other results indicate that the presence of dew does not reduce the rate of ozone deposition, contradicting to model assumptions, and that model assumptions involving the dependency of stomata upon environmental temperature are unnecessary. The effects of measurement errors and biases, arising from the presence of the roughness sublayer and possible photochemical reactions, are also discussed. A simpler model for ozone surface deposition (at least for the San Joaquin Valley) is proposed and evaluated.

1. Introduction

A major sink for the destruction of tropospheric ozone is the gaseous dry deposition onto soil and plant surfaces [*Lefohn*, 1992]. In sufficiently high concentrations, ozone can deleteriously affect plant stomatal functioning, photosynthesis, and a variety of other physiological activities [*Treshow and Anderson*, 1989]. The California Ozone Deposition Experiment (CODE) is a program of observations and modeling to improve grid-based photochemical model estimates of the rate of removal of tropospheric ozone at the Earth's surface. CODE supports a larger air quality measurement and modeling effort comprising the San Joaquin Valley Air Quality Study (SJVAQS) and Atmospheric Utilities Signatures, Predictions, and Experiments (AUSPEX) [*Ranzieri and Thuillier*, 1991]. These efforts are now joined as SJVAQS/AUSPEX Regional Model Adaptation Project (SARMAP). The primary purpose of the present study is to compare predictions of a surface conductance model of ozone deposition, formulated by *Wesely* [1989] and used in the regional acid deposition model (RADM) [*Chang et al.*, 1987], with surface conductance data derived from eddy correlation measurements taken at three sites in the San Joaquin Valley of California. A secondary intention of this paper is to present and test a surface conductance model which better describes the CODE data than the original *Wesely* [1989] formulation.

Because this work is modeling related, there are three important concerns which need to be addressed before continuing. First, the SARMAP air quality model (SAQM) is being used in conjunction with the RADM surface deposition module to model the air quality of the San Joaquin Valley [*Chang et al.*, 1993; *Ranzieri and Thuillier*, 1993]. Therefore it is important that the surface uptake of ozone be accurately simulated within the model domain. Second, the *Wesely* [1989] ozone deposition model was not designed for specific sites of the San Joaquin Valley of California. Rather, it is intended to provide long-term, large area estimates of ozone uptake over the eastern United States. These two regions of the United States have very different climates, rain fall patterns, and plant cover. Consequently, we have no (a priori) reasons to expect the Wesely deposition model to simulate the CODE data very well. Third, the motivation for this study is the need to evaluate the importance of ozone deposition within an air quality modeling context. As such,

[1]U.S. Department of Agriculture/Forest Service, Fort Collins, Colorado.
[2]California Air Resources Board, Sacramento, California.
[3]National Center for Atmospheric Research, Boulder, Colorado.
[4]University of California, Kearney Agricultural Center, Parlier, California.
[5]Atmospheric Environment Service, Downsview, Ontario, Canada.
[6]NASA Ames Research Center, Moffett Field, California.
[7]Department of Land, Air, and Water Resources, University of California, Davis.

Copyright 1994 by the American Geophysical Union.

Paper number 93JD03267.
0148-0227/94/93JD-03267$05.00

CHAPTER IV

Pergamon

Atmospheric Environment Vol. 29, No. 21, pp. 3181–3188, 1995
Elsevier Science Ltd
Printed in Great Britain

1352–2310(94)00330–0

SURFACE CONDUCTANCES FOR OZONE UPTAKE DERIVED FROM AIRCRAFT EDDY CORRELATION DATA

W. J. MASSMAN,* J. I. MACPHERSON,† A. DELANY,‡ G. DEN HARTOG,§ H. H. NEUMANN,§ S. P. ONCLEY,‡ R. PEARSON JR,‖ J. PEDERSON¶ and R. H. SHAW**

*USDA/Forest Service, 240 W. Prospect, Fort Collins, CO 80526, U.S.A.; †Institute for Aerospace Research, National Research Council, Ottawa, Ontario, Canada K1A 0R6; ‡National Center for Atmospheric Research, P.O. Box 3000, Boulder, CO 80307, U.S.A.; §Atmospheric Environment Service, 4905 Dufferin Street, Downsview, Ontario, Canada M3H 5T4; ‖MS-245-5, NASA Ames Research Center, P.O. Box 1000, Moffett Field, CA 94035-1000, U.S.A.; ¶California Air Resources Board, P.O. Box 2815, Sacramento, CA 95812, U.S.A.; **Department of Land, Air and Water Resources, University of California, Davis, CA 95616, U.S.A.

(*First received* 18 *November* 1993 *and in final form* 22 *September* 1994)

Abstract—Plants and soils act as major sinks for tropospheric ozone, especially during daylight hours when plant stomata are thought to provide the dominant pathway for ozone uptake. The present study, as part of the larger California Ozone Deposition Experiment, uses aircraft eddy covariance measurements taken during the summer of 1991 in the San Joaquin Valley of California to estimate the surface conductance for ozone uptake. To explore for possible sources of discrepancies between the aircraft-derived and tower-based surface conductances a comparison is first made between tower-based fluxes and aircraft fluxes at three tower-based sites. On the average the momentum and surface energy fluxes (sensible and latent heat) observed between 30 and 33 m altitude with an aircraft agreed to within $\pm$ 10% with simultaneously measured tower-based fluxes (observed between 4 and 10 m at a vineyard, a cotton and a grassland site). However, comparisons of the aircraft- and tower-based ozone fluxes indicate that between about 4 and 33 m there is an average loss of ozone flux with height of about 18%. It is suggested that either (or both) soil NO emissions or entrainment of ozone free air at the top of the mixed layer may be responsible for this relatively larger discrepancy in the ozone fluxes. Nevertheless, in spite of any relatively larger uncertainties associated with the ozone flux, the tower-based and aircraft-based conductances are in good agreement. The aircraft-derived conductances display a similar magnitude and range of variation as the tower-based conductances and the regression coefficient between the two sets of conductances is 0.9 $\pm$ 0.08. Therefore, results from this study suggest that the aircraft can be used to estimate surface conductances of ozone deposition; however, these conductances are subject to large uncertainties.

Key word index: Ozone dry deposition, San Joaquin Valley, aircraft and tower eddy covariance fluxes, ozone surface conductances.

INTRODUCTION

A major sink of tropospheric ozone is its gaseous dry deposition onto plant and soil surfaces (Lefohn, 1992). For many vegetated surfaces plant stomata are thought to be the major pathway for ozone destruction (e.g. Wesely, 1989). Consequently, to accurately model ozone uptake by plants and soils it is necessary to have reliable observations of the surface conductance to ozone destruction. Although there have been many previous aircraft studies of ozone deposition (e.g. Lenschow *et al.*, 1980, 1981, 1982, 1988; Greenhut, 1983; Kawa and Pearson, 1989a, b; Godowitch, 1990; Ritter *et al.*, 1990, 1992, 1994), none were intended to focus as heavily on ozone surface conductance as was the California Ozone Deposition Experiment (CODE). The primary purpose of the present study, a part of the larger CODE, is to evaluate aircraft-derived surface conductances to ozone uptake and to compare them with ozone surface conductances determined from tower data. A secondary, but important, purpose of this study is to assess the relative importance that different plant species in the San Joaquin Valley can have upon the surface conductances to ozone deposition.

MATERIALS AND METHODS

Experimental data and instrumentation

Between 8 July 1991 and 6 August 1991 the San Joaquin Valley Air Pollution Study Agency (in collaboration with the Pacific Gas and Electric Company, the Electric Power Research Institute and the California Air Resources Board)

CHAPTER IV

Global Change Biology (1995) 1, 183–198

Estimating canopy conductance to ozone uptake from observations of evapotranspiration at the canopy scale and at the leaf scale*

W.J. MASSMAN† and D.A. GRANTZ‡

†*Rocky Mountain Forest and Range Experiment Station, 240 W. Prospect, Fort Collins, CO 80526, USA;* ‡*University of California-Riverside, Kearney Agricultural Centre, 9240 S. Riverbend Avenue, Parlier, CA 93648, USA*

Abstract

Stomatal uptake by vegetation is often the major sink for the destruction of tropospheric ozone. Using data obtained during the summer of 1991 at a grape vineyard and a cotton field in the San Joaquin Valley of California, we compare canopy (stomatal) conductances to ozone estimated (1) from eddy covariance ozone flux data (2) from eddy covariance evapotranspiration data and (3) by scaling leaf transpirational conductance to the canopy level using a canopy radiative transfer model. These simultaneous data, obtained at two levels of biological organization and for two trace gases, allow us to contrast the pathways for canopy–atmosphere exchange of water vapour and ozone, to evaluate limitations to scaling from leaf to canopy, and to predict ozone uptake parameters from those governing transpiration. At the vineyard site the eddy covariance ozone results underestimate the ET-based (eddy covariance and leaf scaling) approaches between 25% and 36%. At the cotton site the ozone-based results overestimate the ET-based approaches between 9% and 62%. A number of modelling and measurement uncertainties are of appropriate magnitude to reconcile these estimates. Some of the possible causes for these discrepancies that are discussed include NO effects, mesophyll resistances to ozone uptake and flaws in the K-theory (first-order closure) approach on which the canopy-scale analysis is based. Nevertheless, both canopy and single leaf measurements of conductance for water vapour provide acceptable estimates of conductance for ozone, but further experiments in which all are measured simultaneously are suggested.

Keywords: canopy conductance, leaf-to-canopy scaling, evapotranspiration, ozone deposition

Received 30 March 1995; revision accepted 8 June 1995

1 Introduction

Ozone, when taken up through plant stomata, can impair stomatal functioning, photosynthesis and a host of other plant physiological activities (Treshow & Anderson 1989). These plant responses in turn affect the release of water vapour, the uptake of CO_2 and the release of volatile organic hydrocarbons. Because plant stomata are often the major pathway for the dry deposition and removal of surface (tropospheric) ozone (Reich 1987; Lefohn 1992) and because tropospheric ozone is expected to increase (at least in the Northern Hemisphere) (Thompson 1992; Turco 1992), observational and modelling studies of dry deposition of ozone are likely to become increasingly important for understanding plant response to ozone and the impact that this can have on tropospheric chemistry.

The present study, part of the California Ozone Deposition Experiment (CODE), compares canopy (stomatal) conductances to ozone estimated from (a) eddy covariance ozone flux data, (b) eddy covariance evapotranspiration (ET) data, and (c) leaf-level measurements of transpirational conductance scaled to the canopy level using a radiative transfer model. We test the hypothesis that bulk canopy stomatal uptake of ozone scales in a predictable manner to canopy transpiration determined

*The use of trade and company names in this paper is for the benefit of the reader; such use does not constitute an official endorsement or approval of any service or product by the US Department of Agriculture or by the California Air Resources Board to the exclusion of others that may be suitable.

Correspondence: W.J. Massman, fax +1-970-4981010, e-mail/s = w.massman/ou1 = s28a@mhs-fswa.attmail.com; D.A. Grantz, fax +1-209-8912593, e-mail: david@uckac.edu.

© 1995 Blackwell Science Ltd.

Chapter VI

Final Data Report for the California Ozone Deposition Experiment

INTRODUCTION

This chapter, the final data report for ground-based data sets of the California Ozone Deposition Experiment, documents changes made after the original reports were issued and discusses some of the assumptions on which the data analyses are based. The ground-based data are documented in four separate reports: one for each of the three eddy covariance tower sites (Delany et al., 1993; The Air Quality Processes Research Division, 1993; and Shaw and Paw U, 1992) and a fourth that documents the biophysical measurements made at each of these three tower sites (Grantz, 1992). All reports are available from Jim Pederson of the California Air Resources Board (CARB) or Bill Massman of the USDA/Forest Service.

UPDATE OF ORIGINAL NCAR REPORT

The complete (20 Hz) cotton data set is available at the National Center for Atmospheric Research (NCAR). The final data set, comprised of half-hourly values of selected data fields and documented in the NCAR report (Delany et al., 1993), is derived from the complete data set. An intermediate cotton data set is described and documented in Tables 1–3 of this report. This intermediate data set is contained in three files, designated "Scalar5.dat", "Mom.dat", and "Other.dat" and was derived from the complete data set.

Included in the intermediate and final data sets is the final ozone flux sensor calibration. This ozone calibration was derived after the experiment because the usual *in situ* method of calibrating the ozone flux sensor failed during the experiment. Temperatures within NCAR's housing for the slow-response ozone monitor were too high for it to work properly. Consequently, the ozone flux sensor was calibrated against PG&E's ambient ozone monitor by adjusting 5 minute raw averages from NCAR's complete data set to match the 1-hour averaged ozone measurements obtained with the ambient ozone monitor. This post-experiment calibration seems to give reasonable results and is discussed in detail by Pearson et al. (1996).

Included in the intermediate and final data sets are several corrections to the eddy covariance flux data and the sonic anemometer data. These include despiking of all of the raw sonic anemometer signals, a tilt correction to the sonic data to correct for small misalignments of the vertical axis, a maximum 5% flow distortion correction to one of the 3-axis sonic anemometers (Atmospheric Technology Incorporated — ATI), and a coordinate rotation in the horizontal plane so that all flux data are defined in the direction of the mean wind.

The final last section of this chapter lists the measured volumetric soil moisture for the cotton site from 7 July 1991 through 7 August 1991.

FINAL DATA FILES - FORMATS AND DISCUSSION

The CODE data for the 3 ground sites are available on 3.5" diskettes and are space-delimited ASCII files. The formats for these files are: [5(i8), 65(f12.3)] for the grape site*; [i2, i3, i3, i2, i2, f8.2, 4f7.2, f8.2, f8.3, f7.2, f8.2, f8.3, f9.3, 6f7.2, f8.3, 2f7.2, 2f6.1, 6f8.3] for the grassland site; and [1x, i2, 1x, i3, 2(1x,i8), 2(1x,i2), 1x, i1, 75(1x,e12.6)] for the cotton site. The corresponding data fields are defined in each of the appropriate reports. These format statements were used in a Fortran program, Calif1.f77, developed by the author for the analyses of the CODE data to extract the site-specific data for further analyses. The publication by Massman et al. (1994) provides details of the results for some of these analyses.

Also included in these analyses are the wetness sensor data discussed by Grantz (1992),which are primarily intended for dew detection. Of the three ground sites, only the grape site included wetness sensors as part of the instrumentation protocols. The biophysical study of Grantz (1992), which was initiated after the original protocols had been established, specifically included wetness sensors to complete the ground-based data sets at the cotton and grassland sites. These wetness sensors are used to augment the original wetness sensor data at the grape site. In Calif1.f77, Grantz's wetness sensor data is implemented into the computer code using the variable "wts" (for wetness) as an original data field. The biophysical wetness data was programmed directly into the computer code because it was originally recorded at 20 minute intervals rather than at the 30 minute recording interval used at the tower sites.

Calif1.f77 also includes two logical variable arrays "kp" and "kpco2". These logical variables are used to eliminate invalid data and to remove outliers in the ozone and carbon dioxide data that were not eliminated when the data were screened for wind direction and/or excessively large values of the Monin-Obukhov stability parameter (z/L), see Massman et al. (1994). Finally, Calif1.f77 also does a small amount of internal calculation for several of the data fields. These internal calculations are used to compute the relative humidity and/or saturation vapor pressure so that the humidity data are consistent between each of the tower sites. The calculations also insert interpolated or extrapolated data values for the heat and moisture fluxes, some of the various radiometer data, the ambient pressure fields and, various temperature fields.

*The latest vineyard data set was released July 1994 and has a slightly different format than the one used in this report. This newest data set eliminates some computational errors that occurred when the previous version was created from the raw (10Hz) data set. However, none of the changes should have any significant impact on results of earlier analyses. This latest vineyard data set is also available from Jim Pederson of the CARB.

Table 1. Header for file Scalar5.dat - all half-hourly averaged data.

PDT u.scalar5 dir.scalar5 w.scalar5 c.scalar5 t.scalar5 q_h2o_uv.scalar5 co2.scalar5 h2o.scalar5 o3.scalar5 u:u.scalar5 u:v.scalar5 u:w.scalar5 u:c.scalar5 u:t.scalar5 u:q_h2o_uv.scalar5 u:co2.scalar5 u:h2o.scalar5 u:o3.scalar5 v:v.scalar5 v:w.scalar5 v:c.scalar5 v:t.scalar5 v:q_h2o_uv.scalar5 v:co2.scalar5 v:h2o.scalar5 v:o3.scalar5 w:w.scalar5 w:c.scalar5 w:t.scalar5 w:h2o.scalar5 w:co2.scalar5 w:q_h2o_uv.scalar5 w:o3.scalar5 c:c.scalar5 c:t.scalar5 c:q_h2o_uv.scalar5 c:co2.scalar5 c:h2o.scalar5 c:o3.scalar5 t:t.scalar5 t:q_h2o_uv.scalar5 t:co2.scalar5 t:h2o.scalar5 t:o3.scalar5 q_h2o_uv:q_h2o_uv.scalar5 q_h2o_uv:co2.scalar5 q_h2o_uv:h2o.scalar5 q_h2o_uv:o3.scalar5 co2:co2.scalar5 co2:h2o.scalar5 co2:o3.scalar5 h2o:h2o.scalar5 h2o:o3.scalar5 o3:o3.scalar5 aflag.scalar5 bflag.scalar5 cflag.scalar5 sflag.scalar5 SIGMAi.scalar5 E.scalar5 [illegible]scalar5 H.scalar5 ustar.scalar5 zoL.scalar5 FO3V.scalar5 O3M.scalar5 FO3M.scalar5 FCO2E.scalar5 CO2V.scalar5 o3.slow o3.rxp o3.pmt o3.rxt o3.hv o3.flowno ozonecal

NOTATION CONVENTION

x.scalar5 = the 'x' data field measured on the NCAR scalar tower 5 meters above the surface
x:y.scalar5 = half hourly covariance between x and y data fields

PDT = Pacific daylight time = the beginning of the half-hour at which the data are recorded
u = horizontal wind speed (first field) otherwise
= streamwise component of the horizontal wind (m/s)
v = cross wise component of the horizontal wind (m/s)
dir = wind direction (degrees)
w = vertical wind speed (m/s)
c = speed of sound (m/s)
t = temperature (C)
q_h2o_uv = mass concentration of ambient water vapor from the uv hygrometer (mg/m3)
co2 = mass concentration of ambient carbon dioxide (mg/m3)
h2o = mass concentration of ambient water vapor from the krypton hygrometer (mg/m3)
o3 = volume concentration of ambient ozone (ppbV)

aflag = despiking flag for the 'a' axis of the University of Washington sonic anemometer (fraction of total number of observations that were despiked)
bflag = same as aflag except for the b axis
cflag = same as aflag except for the c axis
sflag = same as the a flag except for the speed of sound channel

o3.slow = diagnostic channel for the ozone sensor (probably meaningless)
o3.rxp = diagnostic channel for the ozone sensor (probably meaningless)
o3.pmt = diagnostic channel for the ozone sensor (probably meaningless)
o3.rxt = diagnostic channel for the ozone sensor (probably meaningless)
o3.hv = diagnostic channel for the ozone sensor (probably meaningless)
o3.flowno = diagnostic channel for the ozone sensor (probably meaningless)
ozonecal = final ozone sensor calibration

All other fields are the same as in the NCAR report

Table 2. Header for file Mom.dat - all half-hourly averaged data.

PDT u1.5 v1.5 u3 v3 u5 v5 u7.5 v7.5 u10 v10 spd1.5 spd3 spd5
spd7.5 spd10 dir1.5 dir3 dir5 dir7.5 dir10 u.mom10 dir.mom10 w.mom10
c.mom10 t.mom10 u:u.mom10 u:v.mom10 u:w.mom10 u:c.mom10 u:t.mom10
v:v.mom10 v:w.mom10 v:c.mom10 v:t.mom10 w:w.mom10 w:c.mom10 w:t.mom10
c:c.mom10 c:t.mom10 t:t.mom10 uflag.mom10 vflag.mom10 wflag.mom10
cflag.mom10 H.mom10 ustar.mom10 u.mom5 dir.mom5 w.mom5 c.mom5 t.mom5
u:u.mom5 u:v.mom5 u:w.mom5 u:c.mom5 u:t.mom5 v:v.mom5 v:w.mom5 v:c.mom5
v:t.mom5 w:w.mom5 w:c.mom5 w:t.mom5 c:c.mom5 c:t.mom5 t:t.mom5
aflag.mom5 bflag.mom5 cflag.mom5 sflag.mom5 H.mom5 ustar.mom5

NOTATION CONVENTION

xa = the 'x' data field measured on the profile towers at height 'a' meters above the surface
x.moma = the 'x' data field measured on the momentum tower at height 'a' meters above the surface

ua = East/West component of the wind speed at height 'a' above the surface as measured with the propeller anemometers (m/s)
va = North/South component of the wind speed at height 'a' above the surface as measured with the propeller anemometers (m/s)

uflag.mom10 = despiking flag for the u-axis of the ATI sonic anemometer (fraction of the total number of observations that were despiked)
vflag.mom10 = same as uflag except for the v-axis
wflag.mom10 = same as uflag except for the w-axis

All other fields and notation as in SCALAR.HED and/or the NCAR report

Note that the u and v fields associated with the momentum towers refer to the sonic anemometers (u = mean wind speed in the direction of flow and v = the cross wind component), while u and v fields associated with the profile towers refer to the propeller anemometers as defined above

Table 3. Header for file Other.dat - all half-hourly averaged data.

PDT p1 p2 p3 p pkPa tdry.5 twet.5 tdry1.5 twet1.5 tdry3 twet3 tdry5 twet5 tdry7.5 twet7.5 tdry10 twet10 e.5 e1.5 e3 e5 e7.5 e10 q.5 q1.5 q3 q5 q7.5 q10 net psp.out psp.in pyg.out pyg.in T.srfc pyg.out.dome pyg.out.case pyg.in.dome pyg.in.case net.canopy par Td.canopy Tr.canopy T.ridge.8cm T.furrow.8cm T.7cm.Nf T.7cm.r T.7cm.Sf T.5cm.Nf T.5cm.r T.5cm.Sf T.3cm.Nf T.3cm.r T.3cm.Sf T.1cm.Nf T.1cm.r T.1cm.Sf G.8cm.Nf G.8cm.r G.8cm.Sf G.Nf G.r G.Sf G Tcosmos Tmarigold Tragwort

NOTATION CONVENTION

p1 = first of three pressure measurements (mb)
p2 = second of three prressure measurements (mb)
p3 = third of three pressure measurements (mb)
p = average pressure measurement = (p1+p2+p3)/3 (mb)
pkPa = average pressure measurement (kiloPascals)

tdrya = dry bulb temperature measured on the profile tower at height 'a' meters above the surface (C)
tweta = wet bulb temperature meaasure on the profile tower at height 'a' meters above the surface (C)

Tcosmos = internal temperature of cosmos, a signal relay box (C)
Tmarigold = internal temperature of marigold, a signal relay box (C)
Tragwort = internal temperature og ragwort, a signal relay box (C)

All other fields and notation as in the NCAR report

FLUX CORRECTIONS

The final data sets and/or the analysis program Calif1.f77 include several corrections to the fluxes measured at each of the three sites. These corrections include shadowing by the sonic anemometer transducer heads, the Webb-Pearman-Leuning (WPL) correction for density variations, oxygen corrections to the Krypton hygrometer used at the cotton site, a water vapor correction to the ozone sensor used at the cotton site, a gain correction for the CO_2 used at the cotton site and instrument geometry and separation corrections at all three sites.

Shadowing corrections

Neither the sonic anemometer used at the grape site nor the University of Washington sonic used at the cotton site were corrected for shadowing. These instruments are designed to minimize shadowing effects and current estimates suggest that their designs cause less than 2% error in the flux measurements. The ATI sonic used at the cotton site has a maximum 5% correction due to shadowing. The exact correction is a function of the wind direction relative to the axis of symmetry of the sonic anemometer. Flux measurements made at the grass site were made with a single axis sonic anemometer and again shadowing effects are probably insignificant. However, the grassland site also deployed several 3-axis ATI sonics (with a different design than the ones used at the cotton site) that can have significant shadowing effects. Since the friction velocity, u_*, was estimated with this sonic it is likely that the stability parameter, z/L, is overestimated. The exact correction is both wind direction and wind speed dependent. While it is possible that z/L is overestimated by as much as 50% the average overestimation is probably less. No shadowing correction was applied to this instrument for lack of a precise algorithm.

Webb-Pearman-Leuning and similar corrections

The WPL correction arises from atmospheric density fluctuations associated with heat and/or moisture fluxes. Variants of this correction are normally applied to most measured fluxes of trace gases. The final data sets for the grape and grassland sites include the WPL correction to the water vapor, CO_2 and ozone fluxes as discussed and documented in their corresponding reports. The water vapor fluxes at both sites include the heat correction term ($E_{true} = [1 + (m_a/m_v)(\rho_v/\rho_a)][E_{measured} + \rho_v\overline{w'T'}/T]$). The CO_2 flux (grassland only) and ozone flux (both sites) have only the water vapor flux correction ($Fc_{true} = Fc_{measured} + (m_a/m_v)(\rho_c/\rho_a)\overline{w'\rho_v'}$) applied. At the grape site the WPL correction for the CO_2 flux includes the heat flux correction ($[1+(m_a/m_v)(\rho_v/\rho_a)]\rho_c\overline{w'T'}/T$) which is added to the water vapor flux correction. (Here the fluxes refer to mass fluxes, ρ refers to density, m refers to molecular weight, and the subscripts correspond to dry ambient atmosphere "a", to water vapor "v" and to ozone or CO_2 "c". All other symbols are defined in the final reports.) The heat flux correction term is not always included for eddy covariance flux measurements made with a closed path sampling system. For this case it is usually assumed that by the time the gas sample reaches the analyzing chamber the temperature

fluctuations have been damped out by the intake tube. Therefore, the heat flux correction is sometimes ignored.

The final data set for the cotton site includes (a) the WPL correction and the oxygen correction to water vapor fluxes measured with the Krypton hygrometer; (b) a multiplier of 1.42 to the calibration of the CO_2 flux instrument that corrects an electronic gain problem discovered after the experiment was performed; and (c) a water vapor correction to the ozone data. The final data set does not include the WPL correction for the CO_2 flux data. This last correction is in the analysis program Calif1.f77. Before documenting the WPL correction to the CO_2 flux there are three important comments concerning the other corrections that need to be made. First, the ozone sensor used at the cotton site does not require the WPL correction. Second, the oxygen correction to the Krypton hygrometer is given as $\kappa\rho_v\overline{w'T'}/T$ where κ is calibration factor that varies with background pressure. Third, the water vapor correction for the ozone sensor at the cotton site would normally be applied to both fluxes and concentrations. However, because the ozone sensor was recalibrated using the ambient ozone concentrations measured with the PG&E instrument no correction is necessary to the ozone concentrations and only an abbreviated form is necessary to the ozone fluxes. This water vapor correction is $\mathrm{Fc}_{true} = \mathrm{Fc}_{measured} + \mu(\rho_c/\rho_v)\overline{w'\rho_v'}$, where the factor μ is 5, but it can vary between 4 and 6.

Finally, the WPL correction to the CO_2 instrument at the cotton site is $\mathrm{Fc}_{true} = \mathrm{Fc}_{measured} + [(m_a/m_v)(\rho_c/\rho_a) - \beta/\alpha]\overline{w'\rho_v'} + [1 + (m_a/m_v)(\rho_v/\rho_a)]\rho_c\overline{w'T'}/T$, where the calibration factor β/α is 0.0016, but it is very uncertain and can contribute significantly to the correction term. Although the CO_2 flux data can seem reasonable, there is still considerable doubt about its exact calibration and performance. The ambient CO_2 concentration data is untrustworthy and many of the CO_2 fluxes had to eliminated within Calif1.f77.

Corrections due to instrument design and separation

The corrections associated with instrument design and separation are not routinely done. However, they are included in the analysis program Calif1.f77. The exact corrections used in Calif1.f77 are given in the following two tables.

Table 4. *Flux corrections resulting from instrument design and separation during unstable atmospheric conditions.*

Flux	Cotton Site	Grape Site	Grassland Site
Ozone	1.03	1.04	1.07
Water Vapor	1.02	1.02	1.08
Heat	1.02	1.02	1.02
CO_2‡	1.03	1.04	1.08

‡ Flux corrections applied between the hours of 9am and 5pm only.

Table 5. *Flux corrections resulting from instrument design and separation during stable atmospheric conditions.*

Flux	Cotton Site	Grape Site	Grassland Site
Ozone	1.03+0.040z/L	1.04+0.050z/L	1.07+0.040z/L* 1.07+0.040z/L+0.013(u−1)z/L†
H_2O	1.02+0.035z/L	1.02+0.045z/L	1.08+0.0925z/L
Heat	1.02+0.035z/L	1.02	1.02+0.015z/L* 1.02+0.015z/L+0.005(u−1)z/L†
CO_2‡	1.06* 1.06+0.021(u−1)†	1.15	1.265

* Used only when wind speed, u, is < 1 m/s.

† Used only when wind speed, u, is ≥ 1 m/s.

‡ Flux corrections are applied between the hours of 11pm and 4am only.

These corrections were developed from the more complex methods outlined in Zeller et al. (1989) and Massman et al. (1990). For unstable atmospheric conditions these corrections are small and agree with estimates derived from spectra (The air quality research division, 1993). For unstable conditions these corrections are significantly larger. It is important to note that when analyzing the final data sets, $z/L \leq 1$ was imposed because larger values of z/L were correlated with outliers and/or questionable flux data. When this constraint on z/L is combined with the fact that wind speeds (u in Table 5) were light during the stable conditions, the result is that the corrections of stable conditions are usually less than 18%. In general the flux corrections for stable and unstable conditions are designed to match at neutral ($z/L = 0$) atmospheric conditions, except for the CO_2 flux. The analysis of the CO_2 is different from the other fluxes because they were partitioned between daylight hours (9am through 5pm) when unstable conditions occur and the nighttime hours (11pm through 4am) when stable conditions occur. This partitioning was done to insure that the soil CO_2 respiration could be studied without simultaneous canopy photosynthesis. Consequently, transitional hours were not included in the analysis.

A similar analysis was done for the momentum flux, but these corrections were not applied to the data. Momentum flux was not corrected because of the large uncertainty about how shadowing may have influenced the momentum flux observed at the grassland site. Since one data set could not be reliably corrected it was decided not to correct any of the momentum fluxes. Nevertheless, the correction had it been applied would not likely have exceeded +10%. Because momentum flux (and therefore friction velocity) were not corrected, z/L was not corrected either for any of the sites. Had z/L been corrected for the design and separation effects, the correction would have been no more than $\pm$ 10% at any of the sites and usually much less.

DAILY SOIL MOISTURE - COTTON SITE

Table 6 reports the daily volumetric (or volume fraction) soil moisture, θ, for the cotton site. These data were obtained with the clod method for both the furrow between the rows of cotton plants and the soil ridges where the plants were growing. On the few days that θ was not measured, its value was estimated by linear interpolation or by a reasonable approximation (day 213 only).

Table 6. *Daily volumetric soil moisture for the cotton site.*

Day of Year	Calendar Date	θ ridge	θ furrow
188	July 7	0.248	0.410
189	July 8	0.221	0.343
190	July 9	0.213	0.254
191*	July 10	0.198	0.223
192	July 11	0.184	0.192
193*	July 12	0.185	0.150
194	July 13	0.186	0.109
195	July 14	0.150	0.123
196	July 15	0.144	0.087
197	July 16	0.133	0.077
198	July 17	0.127	0.077
199	July 18	0.121	0.078
200*	July 19	0.120	0.073
201*	July 20	0.118	0.068
202*	July 21	0.116	0.063
203	July 22	0.115	0.058
204	July 23	0.101	0.068
205	July 24	0.092	0.073
206	July 25	0.107	0.065
207*	July 26	0.103	0.064
208*	July 27	0.099	0.062
209*	July 28	0.095	0.061
210	July 29	0.091	0.060
211	July 30	0.085	0.062
212	July 31	0.091	0.063
213†	August 1	0.090	0.060
214	August 2	0.228	0.374
215	August 3	0.235	0.380
216	August 4	0.201	0.378
217	August 5	0.278	0.162
218	August 6	0.230	0.150
219	August 7	0.230	0.150

* θ linearly interpolated.

† The cotton field was irrigated about 3pm. The values of θ shown are approximate and do not reflect any additional soil moisture resulting from the irrigation.

APPENDIX I

A warning to all ASTER users

From Tom Horst - November 28, 1995

We have found that the AIR (Atmospheric Instrumentation Research) fine-platinum-wire temperature sensor, which has been used by ASTER, has reduced response at high frequencies. This is caused by the thermal lag of the copper wire helix that is used (indirectly) to support the platinum wire. The time constant of the copper helix is roughly 5 sec and thus its temperature response is attentuated at frequencies above 0.01 Hz. However, the thermal lag of the copper helix only affects a fraction of the length of the platinum wire, and therefore the attentuation of the PRT response is approximately independent of frequency above say 0.1 Hz. As a consequence the slope of the spectra and cospectra in the inertial range look correct (even though the amplitude is too small), which is one of the reasons why we did not notice this problem sooner.

Our initial estimate is that the sensible heat flux calculated from the AIR PRT data is about 15% too small in unstable conditions and about 30% too small in stable conditions. However, since the attentuation is a complex function of wind direction, wind speed, measurement height and atmospheric stability, we cannot recommend a generic correction to the heat fluxes measured with the PRT. As an alternative, we recommend use of the (virtual) heat fluxes calculated from the virtual temperature determined from speed-of-sound measurements made by the sonic anemometers. Although the virtual heat flux will need to be corrected for the water vapor flux in order to determine the sensible heat flux, note that it is the virtual heat flux, not the sensible heat flux that is required for calculation of the Obukhov length. (In almost every case, either the sonic microprocessor or the ASTER calibration functions that are applied to the raw sonic data make a correction to the sonic data for contamination of the speed-of-sound measurement by the component of the wind normal to the measurement path.)

I'll be glad to answer any questions that you may have .

Tom Horst
Head, Surface and Sounding Systems Facility
Atmospheric Technology Division
NCAR
303-497-8838

REFERENCES CHAPTER VI

Delany, T., S. Semmer, T. Horst, S. Oncley, C. Martin and B. Massman. *The ASTER deployment at the cotton site during the California ozone deposition experiment, 1991 - CODE '91 of the San Joaquin Valley Air Quality Study.* 1993.

Grantz, D.A. *Biophysical measurement to support CODE-91.* 1992. 246 pp.

Massman, W.J., D.G. Fox, K.F. Zeller, and D. Lukens. *Verifying eddy correlation measurements of dry deposition: a study of the energy balance components of the Pawnee Grasslands.* 1990. USDA/Forest Service Research Paper RM-288. 14 pp.

Massman, W.J., J. Pederson, A. Delany, D. Grantz, G. den Hartog, H.H. Neumann, S.P Oncley, R. Pearson, Jr., and R.H. Shaw. *An evaluation of the regional acid deposition model surface module for ozone uptake at three sites in the San Joaquin Valley of California.* 1994. Journal of Geophysical Research, 99: 8281-8294.

Pearson, R., S. Oncley, and A. Delany. *A scalar similarity study based on surface layer ozone measurements over cotton during the California Ozone Deposition Experiment (CODE).* 1996. Journal of Geophysical Research, in press.

Shaw, R.H. and K.T. Paw U. *Observations of dry deposition of ozone in the San Joaquin Valley.* 1992. 34 pp.

The air quality processes research division. *Final documentation report on the vineyard measurements for the San Joaquin Valley Air Pollution Study Agency, Contract 91-2.*, Revision no. 2. 1993. 101 pp.

Zeller, K.F., W. Massman, D. Stocker, D.G. Fox, D. Stedman, D. Hazlett. *Initial results from the Pawnee eddy correlation system for dry acid deposition research.* 1989. USDA/Forest Service Research Paper RM-282, 30 pp.

Chapter VII

Preliminary Investigation of the effects of NO fluxes upon the CODE ozone fluxes

INTRODUCTION

This chapter addresses possible effects that soil Nitrogen Oxide (NO) fluxes can have on the ozone fluxes observed during the CODE. The first section reviews existing literature on soil NO emissions within the central valley and some of the general literature pertinent to estimating soil NO emissions. The second section discusses possible canopy uptake and release of NO. The third and final section uses a simple model to partition the ozone fluxes observed at the cotton site during the CODE into a plant deposition component and an NO titration component.

ESTIMATES OF SOIL NO EMISSIONS WITHIN THE CENTRAL VALLEY

Six studies of soil NO emissions from three sites within or near the central valley of California are summarized below in Table 1. The NO fluxes reported in these studies ranged from near 0.0 ng-N/m^2/s to about 100 ng-N/m^2/s. This large variation could be attributed to variations in soil moisture, soil temperature, the short-term grazing history, the short-term fire history and the timber harvesting practices. The references in Table 1 document the importance of these NO flux regulators.

In addition to the studies outlined in Table 1, there are two other important studies of soil NO emissions. Both Williams et al. (1992) and Yienger and Levy (1995) provide good summaries of existing soil NO flux studies. They develop simple models of soil NO emission rates (or soil NO fluxes) from extensive inventories of flux observations. These two studies differ from those outlined in Table 1 because they model the influence that fertilizers and fertilization rates have on soil NO emissions. The studies in Table 1 discuss the effects of other types of manipulations on the release of NO from soils. For the purposes of estimating possible NO effects on the CODE ozone flux measurements at the cotton site (discussed in the last section of this report) the model developed by Williams et al. (1992)is used.

Table 1. *Measured soil NO flux within or near the central valley of California.*

Ecosystem Description	NO flux (ng-N/m^2/s) Mean	Range	Measurement Date	Reference
Semiarid Chaparral Burned Unburned San Dimas Exp. Forest 60 km NE of LA	 31 13	 6–101 0—35	07/86 & 12/86	Anderson et al. 1988
Semiarid Chaparral Burned/Unburned San Dimas Exp. Forest	14	0—32	12/86	Anderson and Poth 1989
Semiarid Chaparral Burned Unburned San Dimas Exp. Forest	 25 17	 4—60 10–30	06/87	Levine et al. 1988
Oak woodland-grassland Open grassland Oak woodland U of California Sierra Foothills Range Field Station 70 km N of Sacramento	 34 8	 24–42 6–11	02/91	Davidson and Herman 1993
Oak woodland-grassland Open grassland Oak Woodland U of California Sierra Foothills Range Field Station	 2 4	 1—2 1—7	05/93	Herman et al. 1993
Temperate coniferous forest Challenge Exp. Forest near Challenge, CA	7	1–30	08/91	Anderson et al. 1995

NITRIC OXIDE UPTAKE AND RELEASE BY PLANT CANOPIES

Nitric Oxide can be either given off (Farquhar et al. 1983; Klepper 1979) or taken up by plant canopies (Table 2). In general, these studies show that the exchange of NO between the atmosphere and plant canopies is fairly weak. In this report, it is assumed that the soil is the major source for NO and that the CODE cotton canopy removes a small amount of that NO as it passes through the canopy space and into the atmosphere above the canopy. Therefore, the possibility that the cotton plants are actually acting as a source of NO is not discussed.

Table 2 summarizes most of the observations of the uptake rate of NO by plant surfaces and includes the results of a study of bare soil NO uptake (Judeikis and Wren 1978). In general, NO is not strongly taken up by plant canopies and there appears to be little stomatal control. This is particularly evident from the single leaf or single plant studies (LSA in Table 2) because the deposition velocities are small. The whole canopy studies (GSA in Table 2) show relatively higher values of v_d because the amount of absorbing leaf surface is relatively larger than in the LSA studies and because the GSA studies include the soil uptake of NO.

Table 2. *Summary of NO uptake and uptake rates by plants and soil.*

Reference	NO uptake rates and comments Deposition velocity = v_d	Surface/plant type
Hill & Chamberlain 1974	v_d = 1 mm/s (GSA) *	Alfalfa canopy
Judeikis & Wren 1978	v_d = 1.3–1.9 mm/s (GSA)	Bare Soil
Galbally & Roy 1981	v_d = 1–2 mm/s (GSA)	Rural landscape
Skarby et al. 1981	v_d = 0.07 mm/s (LSA) †	Scots pine
Law & Mansfield 1982	v_d = 0.7 mm/s (LSA) Weak stomatal uptake at best Possible mesophyll resistance	Sweet pepper
Granat & Johansson 1983	$v_d < 0.3$ mm/s (LSA)	Spruce and Pine
Galbally et al. 1985	v_d = 1.5 mm/s (GSA)	Grassland/pasture
Saxe 1986	v_d = 0.04–0.4 mm/s (LSA)	8 species of potted house plants
Johansson 1987	$v_d \leq 0.1$ mm/s (LSA)	Scots pine
Kisser-Priesack 1987	Weak uptake of NO by cuticles	Spruce & tomatoes
Wesely et al. 1989	v_d = 1.7 mm/s (GSA) Day v_d = 0.0 mm/s (GSA) Night	Grassland, shrubs and pasture
Herrmann & Jaeschke 1989	$v_d \leq 70$ mm/s (GSA) v_d extremely variable and sometimes negative	Forested landscape
Hanson & Lindberg 1991	v_d = 1.7 mm/s (GSA) from Bennett & Hill 1971	Alfalfa canopy
Neubert et al. 1993	v_d = 0.05–0.55 mm/s (LSA) v_d = 0.20–0.55 mm/s (LSA) Strong stomatal control and possible mesophyll resistance	Tobacco Sunflower

* GSA (per ground surface area)

† LSA (per leaf or needle surface area)

PARTITIONING OZONE FLUXES INTO DEPOSITION AND NO TITRATION

This section outlines a simple model for partitioning the CODE ozone fluxes at the cotton site into a dry deposition component and an NO titration component. The model equations are derived and then applied to the cotton site data.

Assuming steady state conditions, the following flux difference conservation equation is valid for NO-NO_2-O_3 photochemically-driven reactions between the level of measurement (z_m) and the top of the canopy (h) (Fitzjarrald and Lenschow, 1983):

$$\frac{\partial(F_O - F_{NO})}{\partial z} = 0 \tag{1}$$

where F_O = ozone flux and F_{NO} = flux of NO. Integrating between z_m and h yields:

$$F_O(h) = F_O(z_m) + F_{NO}(h) - F_{NO}(z_m) \tag{2}$$

This equation is the basis of the partitioning model. (It is assumed that all fluxes are expressed in ppbV-m/s and that the NO flux is away from the surface and the ozone flux is toward the surface). To accomplish the ozone partitioning $F_{NO}(z_m)$ and F_{NO}(h) are parameterized in terms of $F_{NO}(0)$ and the model of Williams et al. (1992) is used to estimate the soil NO flux. $F_{NO}(0)$.

It is assumed that F_{NO}(h) = q_1[$F_{NO}(0)$ - F_{NO}(canopy)], where F_{NO}(canopy) is the NO uptake rate by the cotton canopy and q_1 is the fraction of the remaining NO flux that escapes to the top of the canopy. Next it is assumed that $F_{NO}(z_m) = q_2 F_{NO}(0)$. Finally, because q_1 is the fraction of NO that reaches the top of the canopy, then (1-q_1) is the fraction of the remaining NO flux that reacts with ozone within the canopy space between the soil surface and the top of the canopy. Therefore, F_O(h) can be partitioned into a deposition component and a NO titration component yielding: F_O(h) = $F_{O,dep}$(h) - [1-q_1][$F_{NO}(0)$ -F_{NO}(canopy)]. Combining the expressions for $F_{NO}(z_m)$, F_{NO}(h) and F_O(h) with equation (2) and solving for $F_{O,dep}$(h) yields:

$$F_{O,dep} = F_O(z_m) + (1 - q_2)F_{NO}(0) - F_{NO}(canopy) \tag{3}$$

The parameter value for q_2 is assumed to be 0.25, (i.e., 25% of the soil NO flux reaches the height at which the ozone is measured). This agrees with the observations of Bakwin et al. (1990) who found that $q_2 = 0.40$ above the Amazon forest and the model calculations of Jacob and Wofsy (1990) who estimated that $q_2 \leq 0.20$ for the same Amazon forest data set. To estimate the canopy uptake rate F_{NO}(canopy) it is assumed that (a) the leaf surface deposition velocity for NO is 0.3 mm/s; (b) the Leaf Area Index of the cotton canopy is about 2.0; and (c) the within-canopy NO concentration is about 10 ppbV which yields a value for F_{NO}(canopy) = 0.006 ppbV-m/s. The value used for v_d assumes that there is no stomatal control regulating NO deposition to plants and relies most heavily on the results of Law and Mansfield (1982) and Saxe (1986). Nevertheless, F_{NO}(canopy) is highly uncertain partly because of the uncertainty in the v_d estimate and because the within-canopy NO concentration is also estimated. Some hourly NO concentrations data taken near the cotton

eddy covariance site suggest that the above canopy NO concentrations are no greater than 3 ppbV most of time which suggests that the within-canopy NO concentration will exceed this observed amount because of its' proximity to the soil (i.e., the NO source). From Williams et al. (1992), $F_{NO}(0) = 0.016\exp(0.071T_s)$ for heavily fertilized soils as is the case for the cotton crop. (T_s = measured soil temperature.) The above analysis does not include data when dew was present.

Using the above model, the measured ozone fluxes, $F_O(z_m)$, were partitioned into plant deposition [$F_{O,dep}$] and NO titration [$(1\text{-}q_2)F_{NO}(0)$ - F_{NO}(canopy)]. Figure 1 shows the NO titration component as a fraction of the total ozone flux as a function of time of day for the period of the CODE. Although there is some diel variation, in general NO reduces the ozone flux to the canopy and soil between 20% and 60% during the daylight hours and nearly 100% at night. The consequences of this additional sink of surface ozone destruction has significant implications for the ozone surface uptake conductances evaluated by Massman et al. (1994). In particular the results of this model suggest that Massman et al. (1994) may have overestimated the cotton surface conductances by between 25% and 50%.

This present model for estimating the influence of soil NO flux on ozone deposition to plants and soil is qualitative. A more complete model along with a more complete data set is necessary for quantitative predictions of the influence that NO-NO_2-O_3 photochemistry can have upon ozone deposition measurements. The design and implementation of a more complete model has been initiated. The new model is one dimensional, includes variable canopy structure, a new formulation for canopy turbulence, and should be capable of simulating the counter-gradient fluxes often associated with the within-canopy profiles of temperature and trace gases. Once the model has been completed, it will be used to recalculate the canopy conductance to ozone using the CODE data.

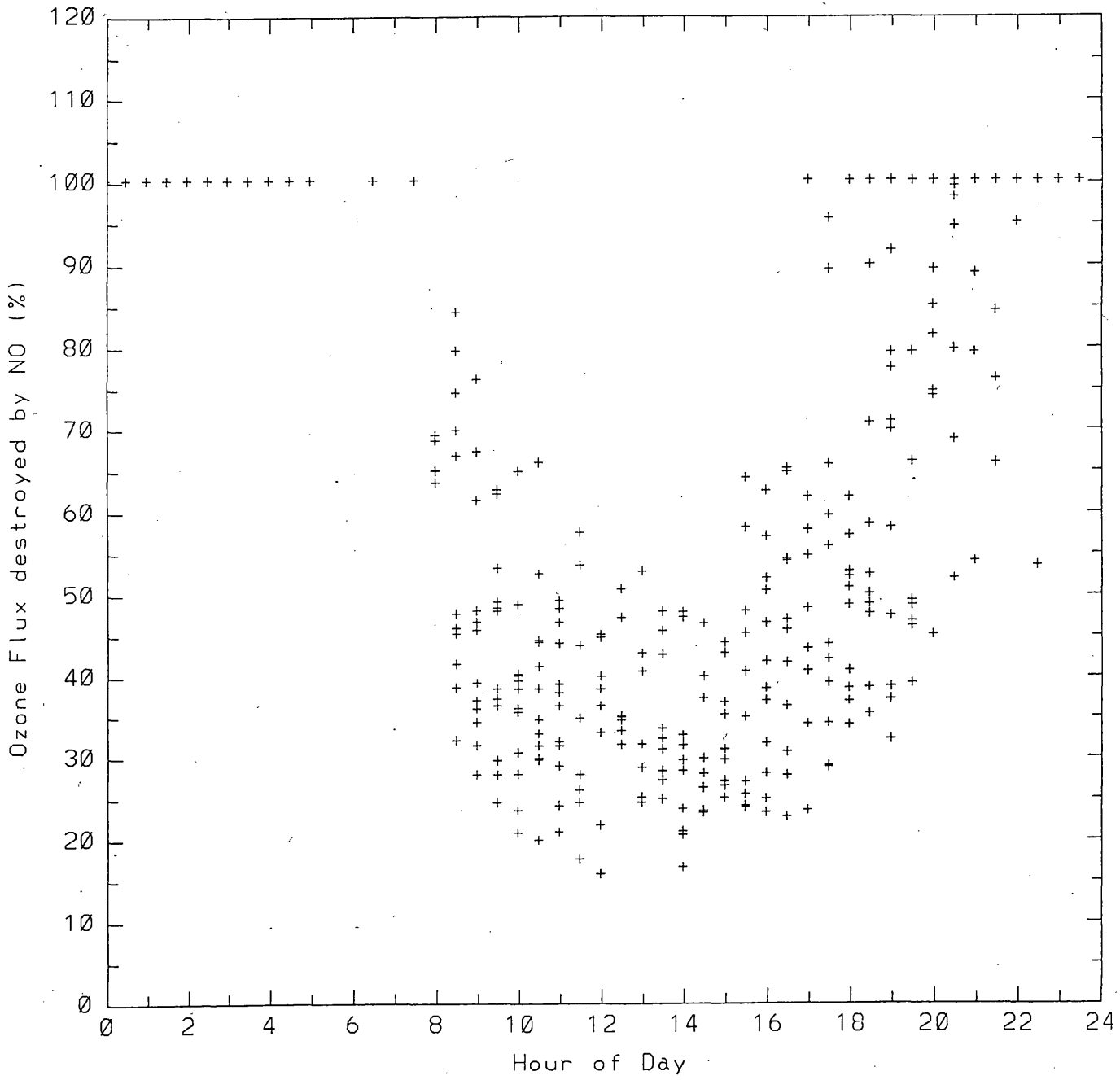
California Ozone Study (Cotton Site)
Ozone Flux destroyed by NO (%)
Hour of Day
0
10
20
30
40
50
60
70
80
90
100
110
120
0
2
4
6
8
10
12
14
16
18
20
22
24

REFERENCES CHAPTER VII

Anderson, I.C., J.S. Levine, M.A. Poth and P.J. Riggan *Enhanced biogenic emissions of nitric oxide and nitrous oxide following surface biomass burning.* 1988. Journal of Geophysical Research, 93: 3893-3898.

Anderson, I.C. and M.A. Poth *Semiannual losses of nitrogen as NO and N_2O from unburned and burned chaparral.* 1989. Global Biogeochemical Cycles, 3: 121-135.

Anderson, I.C., M.A. Poth, S.M. Haase, S.S. Sackett and R.F. Powers. *Regulation of nitric oxide, nitrous oxide, and carbon dioxide emissions from temperate coniferous forest soils disturbed by clearcutting or burning.* 1995. (personal communication from M.A. Poth, 909-276-6571).

Bakwin, P.S., S.C. Wofsy, S-M. Fan, M. Keller, S.E. Trumbore and J.M. DaCosta. *Emission of nitric oxide (NO) from tropical forest soils and exchange of NO between the forest canopy and atmospheric boundary layer.* 1990. Journal of Geophysical Research, 95: 16755-16764.

Bennett, J.H. and A.C. Hill. *Absorption of gaseous air pollutants by a standardized plant canopy.* 1973. Journal Air Pollution Control Association, 23: 203-206.

Davidson, E.A. and D.J. Herman. *Cattle grazing and oak trees as factors affecting soil emissions of nitric oxide from an annual grassland.* 1993. In: *Agricultural ecosystem effects on trace gases and global climate change.* ASA Special Publication no. 55: 109-119. American Society of Agronomy, Madison, WI.

Farquhar, G.D., R. Wetselsaar and B. Weir. *Gaseous nitrogen losses from plants.* 1983. In: J.R. Freney and J.R. Simpson (eds.) *Gaseous loss of nitrogen from plant-soil systems*: 159-180. Martinus Nijhoff/Dr W. Junk Publishers, The Hague.

Fitzjarrald, D.R. and D.H. Lenschow. *Mean concentration and flux profiles for chemically reactive species in the atmospheric surface layer.* 1983. Atmospheric Environment, 17: 2505-2512.

Galbally, I.E. and C.R. Roy. *Ozone and nitrogen oxides in the southern hemisphere troposphere.* 1981. In: J. London (ed.) *Proceedings of the quadrennial international ozone symposium*: 431-438. International Ozone Commission.

Galbally, I.E., C.R. Roy, C.M. Elsworth and H.A.H. Rabich. *The measurement of nitrogen oxide (NO, NO_2) exchange over plant/soil surfaces.* 1981. CSIRO, Division of Atmospheric Research Technical Paper no. 8: 1-23.

Granat, L. and C. Johansson. *Dry deposition of SO_2 and NO_x in winter.* 1983. Atmospheric Environment, 17: 191-192.

Hanson, P.J. and S.E. Lindberg. *Dry deposition of reactive nitrogen compounds: a review of leaf, canopy and non-foliar measurements.* 1991. Atmospheric Environment, 25A: 1615-1634.

Herman, D.J., G.J. Atkins, L.J. Halverson, P.D. Brooks and M.K. Firestone. *Factors related to N-gas production in a temperate annual grassland.* 1993. (personal communication from D.J. Herman, 510-642-6847).

Herrmann, U. and W. Jaeschke. *Determinations of dry deposition of gases over tree tops by measured data and a numerical model.* 1989. In: H.W. Georgii (ed.) *Mechanisms and effects of pollutant-transfer into forests*: 13-20. Kluwer Academic Publishers, Dordrecht.

Hill, A.C. and E.M. Chamberlain Jr. *The removal of water soluble gases from the atmosphere by vegetation.* 1976. In: *Atmosphere-surface exchange of particulate and gaseous pollutants (1974)*: 153-170. Energy Research and Development Administration symposium series, CONF-740921, NTIS, USDoC, Springfield, VA 22161.

Jacob, D.J. and S.C. Wofsy. *Budgets of reactive nitrogen, hydrocarbons, and ozone over the Amazon forest during the wet season.* 1990. Journal of Geophysical Research, 95: 16737-16754.

Judeikis, H.S. and A.G. Wren. *Laboratory measurements of NO and NO_2 deposition onto soil and cement surfaces.* 1978. Atmospheric Environment, 12: 2315-2319.

Johansson, C. *Pine forest: a negligible sink for atmospheric NO_x in rural Sweden.* 1987. Tellus, 39B: 246-438.

Kisser-priesack, G.M., I. Schuenert and G. Gnatz. *Uptake of $^{15}NO_2$ and ^{15}NO by plant cuticles.* 1987. Naturwissenschaften **74**: 550-551.

Klepper, L. *Nitric oxide (NO) and nitrogen dioxide (NO_2) emissions from herbicide-treated soybean plants.* 1979. Atmospheric Environment, 13: 537-542.

Law, R.M. and T.A. Mansfield. *Oxides of nitrogen and the greenhouse atmosphere.* 1982. In: M.H. Unsworth and D.P. Ormrod (eds.) *Effects of gaseous air pollution in agriculture and horticulture*: 93-112. Butterworth Scientific, London.

Levine, J.S., W/R. Cofer III, D.I. Sebacher, E.L. Winstead, S. Sebacher, and P.J. Boston. *The effects of fire on biogenic soil emissions of nitric oxide and nitrous oxide.* 1988. Global Biogeochemical Cycles, 2: 445-449.

Massman, W.J., J. Pederson, A. Delany, D. Grantz, G. den Hartog, H.H. Neumann, S.P. Oncley, R. Pearson Jr, R.H. Shaw. *An evaluation of the regional acid deposition surface module for ozone uptake at three sites in the San Joaquin Valley of California.* 1994. Journal of Geophysical Research, 99: 8281-8294.

Neubert, A., D. Kley, J. Wildt, H.J. Segschneider and H. Forstel. *Uptake of NO, NO_2 and O_3 by sunflower (Helianthus Annuus L.) and tobacco plants (Nicotiana Tabacum L.): dependence on stomatal conductivity.* 1993. Atmospheric Environment, 27A: 2137-2145.

Saxe, H. *Stomatal-dependent and stomatal-independent uptake of NO_x.* 1986. New Phytologist, 103: 199-205.

Skarby, L., C. Bengtson, C-A. Bostrom, P. Grenfelt and E. Troeng. *Uptake of NO_x in Scots Pine.* 1981. Silva Fennica, 15: 396-398.

Wesely, M.L., D.L. Sisterson, R.L. Hart, D.L. Drapcho and Y.I. Lee. *Observations of nitric oxide fluxes over grass.* 1989. Journal of Atmospheric Chemistry, 9: 447-463.

Williams, E.J., A. Guenther and C. Fehsenfeld. *An inventory of nitric oxide emissions from soils in the United States.* 1992. Journal of Geophysical Research, 97: 7511-7519.

Yienger, J.J. and H. Levy II. *Empirical model of global soil-biogenic NO_x emissions.* 1995. Journal of Geophysical Research, 100: 11447-11464.